Accepted Manuscript

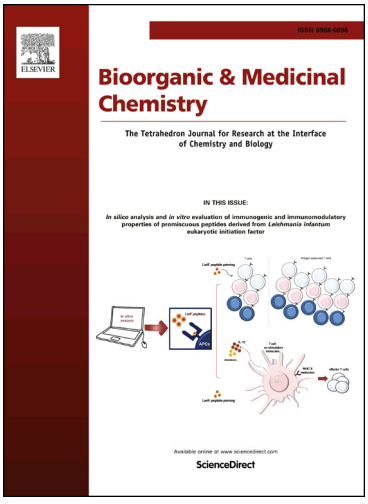

Benzofuran-Dihydropyridine Hybrids: A new class of potential bone anabolic agents

Ram K. Modukuri, Dharmendra Choudhary, Sampa Gupta, K. BhaskaraRao, SulekhaAdhikary, Tanuj Sharma, Mohammad Imran Siddiqi, Ritu Trivedi, Koneni V. Sashidhara

PII: S0968-0896(17)31358-5
DOI: https://doi.org/10.1016/j.bmc.2017.10.018
Reference: BMC 14023

To appear in: *Bioorganic & Medicinal Chemistry*

Received Date: 4 July 2017
Revised Date: 4 October 2017
Accepted Date: 16 October 2017

Please cite this article as: Modukuri, R.K., Choudhary, D., Gupta, S., BhaskaraRao, K., SulekhaAdhikary, Sharma, T., Siddiqi, M.I., Trivedi, R., Sashidhara, K.V., Benzofuran-Dihydropyridine Hybrids: A new class of potential bone anabolic agents, *Bioorganic & Medicinal Chemistry* (2017), doi: https://doi.org/10.1016/j.bmc.2017.10.018

Benzofuran-Dihydropyridine Hybrids: A new class of potential bone anabolic agents

Ram K. Modukuri[†, #], DharmendraChoudhary [‡, #], Sampa Gupta [†], K. BhaskaraRao[†], SulekhaAdhikary[‡], Tanuj Sharma [ϕ], Mohammad Imran Siddiqi[ϕ],RituTrivedi[‡,*]and Koneni V. Sashidhara[†, *]

[†]*Medicinal and Process Chemistry Division,* [‡]*Endocrinology Division,* [ϕ] *Molecular and Structural Biology Division, CSIR-Central Drug Research Institute, (CSIR-CDRI), BS-10/1, Sector 10, Jankipuram Extension, Sitapur Road, Lucknow, 226031, India*

Phone: +91 9919317940; Fax: +91-518-2623405.

Correspondence and requests for materials should be addressed to K.V.S or R.T (e-mail: sashidhar123@gmail.com, kv_sashidhara@cdri.res.in, ritu_trivedi@cdri.res.in)

Part 44th the series, "Advances in drug design and discovery"

[#]These authors contributed equally

Abstract

A series of novel benzofuran-dihydropyridine hybrids were designed by molecular hybridization approach and evaluated for bone anabolic activities. Among the screened library, ethyl 4-(7-(*sec*-butyl)-2-(4-methylbenzoyl)benzofuran-5-yl)-2-methyl-5-oxo-1,4,5,6,7,8-hexahydroquinoline-3-carboxylate (compound **21**) significantly enhanced the ALP production and mineralized nodule formation, which are primary requisites in the process of *in-vitro* osteogenesis. Oral administration of compound **21** at 10 $mg.kg^{-1}day^{-1}$ for two weeks led to restoration of trabecular bone microarchitecture in drill hole fracture model by significantly increasing BV/TV and Tb.N. Furthermore, histological and molecular studies showed compound **21** triggering the new bone regeneration in a drill hole defect site by increasing BMP expression. Furthermore, molecular modeling studies were performed to gain insight into the binding approach, which revealed that both benzofuran and dihydropyridine moieties are essential to show similar binding interactions to fit into the active site of BMP2 receptor, an important target of the osteogenic agents.Our results suggest that compound **21** stimulates BMP2 synthesis in osteoblast cells that promotes new bone formation (~40%) at the fracture site which helps in shorten the healing period.

Keywords: Benzofuran-dihydropyridine hybrids;Alkaline phosphatase; Bone morphogenic protein-2; Molecular hybridization.

Abbreviation: Bone morphogenic protein-2 (BMP2), alkaline phosphatase (ALP), 3-(4, 5-dimethylthiazol-2-yl)-2, 5-diphenyltetrazolium bromide (MTT), Quantitative Real-Time Polymerase Chain Reaction (qRT-PCR), Runt-related transcription factor 2(RUNX2), Alkaline phosphatase (ALP), Collagen type-I (COL1), *Osterix*(*Osx*), Trabecular bone volume/tissue volume (BV/TV), Trabecular number (Tb.N).

1. Introduction

Osteoporosis is a silent skeletal disease that weakens the bone microarchitecture and increases the risk of fragility. It has been recognized as a global health threat and is more prevalent in aged population, mainly postmenopausal women [1]. This disease is initiated because the process of bone resorption overtakes that of new bone formation [2]. Epidemiological studies have estimated that ‘‘by the year 2015, osteoporosis will be responsible for approximately 3 million fractures and $ 25.3 billion in costs each year’’ in the USA [3,4]. At clinical level it is mainly characterized by low bone mineral density and deterioration of the microarchitecture of bone tissue, thereby increasing the risk of fractures [5]. During the post menopause in elderly women, estrogen deprivation enhances osteoclast recruitment and contributes to rapid skeletal loss and bone fragility [6, 7]. Current clinical approaches for osteoporosis fall under two categories, namely anti-resorptive and anabolic agents. Anti-resorptive medications includeestrogens, hormone replacement therapy (HRT), selective estrogen receptor modulators (SERMs), bisphosphonates, and antibody therapy (calcitonin and denosumab) [8]. Although their sites of action may differ, these medications reduce bone loss by decreasing osteoclastic bone resorption [9]. However, most of the medications available in this class are associated with serious side effects (nausea, esophageal, osteonecrosis of the jaw and cancer) and unsatisfactory results [10]. Anabolic agents which stimulate the osteoblastic bone formation and increase the bone mineral density have recently widened the therapeutic options [11]. Teriparatide (a recombinant version of human Parathyroid hormone (PTH)) is the only FDA-approved anabolic agent which reverses the disease by stimulating bone synthesis [12]. However, because of long-term safety and efficacy are unknown, it is prescribed for only two years. Main limiting factors of PTH therapy are its compliance (parenteral route of administration) and development of

osteosarcoma at higher doses, thereby highlighting the need for alternate bone anabolic agents [13,14].

Bone morphogenetic protein 2 (BMP2) is mainly synthesized by bone forming osteoblast cells and it stimulates osteoblasts differentiation, bone generation and regeneration at defecated site [15]. Animal studies confirmed the positive role of recombinant BMP2 in fracture healing [16-17]. In this direction synthesise of BMP2 up regulator like novel molecules may provide new therapeutic agents for the treatment of fracture healing studies.

In current drug discovery, anabolic strategy is an attractive concept for the discovery of new agents to advance the therapy of osteoporosis [18].With this new paradigm, there is a tremendous opportunity to make a significant positive impact on the health and lives of osteoporotic people through the discovery and development of new bone anabolic agents, that enhances both new bone formation (rapid fracture healing property) and also increase the bone mineral density with less adverse effects.

Benzofuran and their derivatives have been found to exhibit different biological and pharmacological activities like anti-tubercular, antibacterial, anti-fungal, anti-inflammatory, anti-depressant etc [19-20]. Owing to their beneficial effects on bone health, they have been a subject of further studies [21-23]. Benzofuran derivatives were reported to exert beneficial effects in the prevention of bone loss (**Figure 1A**) [24]. Interestingly, Kumar *et al.* demonstrated that benzofuran containing non-peptide inhibitor SB-462795 prevents bone loss in both *in-vitro* and *in vivo* animal models (**Figure 1B**) [25]. Recent remarkable work of Guo*et al.* have established the potential of 2-substituted benzofuran derivatives as anovel class of bone anabolic agents that were able to up-regulateBMP2 expression in ovariectomized rats (**Figure 1C**) [26]. In the field of anabolic therapy a small molecule which enhances bone strength and the growth factor could be crucial for the treatment of the osteoporosis. Hence, 2-substituted benzofuran structural moiety was incorporated as one of

the pharmacophoricpartners in our hybridization approach. However, several reports suggest that calcium channel blockers containing dihydropyridine in their molecular makeup stimulate the osteoblast differentiation and have a beneficial effect by reducing fracture risk [27-30]. Interestingly, the studies by Wang *et al.* have suggested that this class of compounds (benidipine) promoted cell proliferation and exhibited osteogenic differentiation at potentially lower concentrations (**Figure 1D**) [31]. Furthermore, Ushijima *et al.* have revealed the protective role of amlodipine against osteoporosis in hypertensive rats (**Figure 1E**) [32]. We have previously developed coumarin-containingdihydropyridine hybrids as a new class of bone anabolic agents, which also underscores the importance of dihydropyridine scaffold against osteoporosis (**Figure 1F**) [33].

Small molecules, which can modulate relevant multiple targets can enhance efficacy and emerge as a better therapeutic candidate. [34-39]. In this study, following the medicinal chemistry hybridization approach a series of compounds belonging to the prototype incorporating pharmacophoric features of benzofuran and 1, 4- dihydropyridinewere synthesized and evaluated *in vitro* and *in vivo* for their intended activity. Figure 1 shows representative potent inhibitors that either contains benzofuran or dihydropyridine in their molecular makeup, along with the structure of our designed prototype.

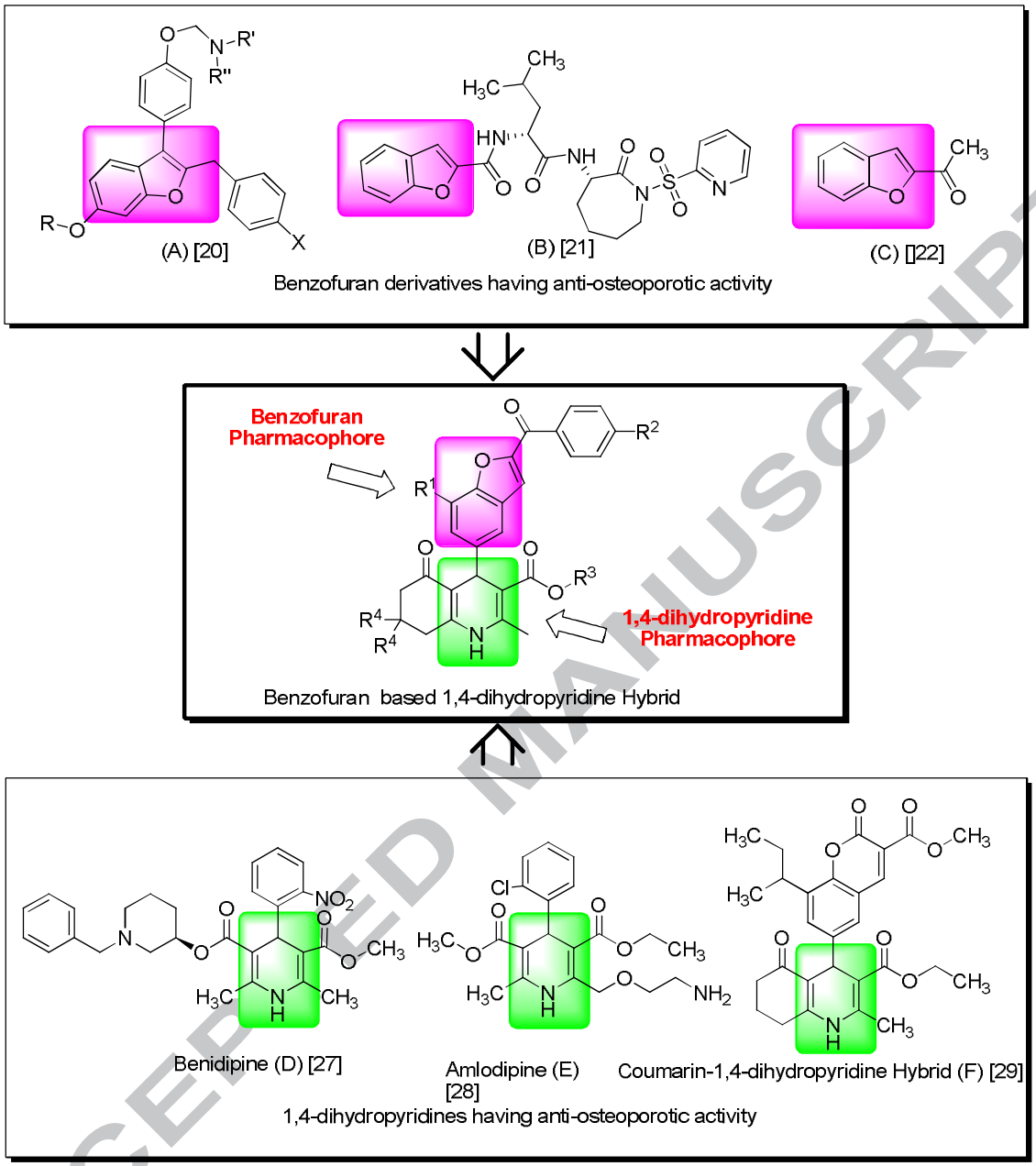

Figure 1: Strategy employed for the design of benzofuran-1,4-dihydropyridine hybrids

2. Results and Discussion

2.1 Chemistry

Interestingly, the anti-osteoporotic potential of benzofuran based 1, 4-dihydropyridines has never been explored. The structural novelty and pharmacophoric importance led us to synthesize 5-substituted benzofuran based hybrids from the benzofurancarbaldehyde key intermediate, which in turn was prepared from our standard dicarbaldehyde substrate using established protocol [40].The synthetic strategy followed is depicted in scheme 1. Initially, the Duff formylation on *ortho*-substituted phenol (**1**-**3**) in the presence of hexamethylenetetramine (HMTA) and trifluoroacetic acid (TFA) at 120 °C gave the corresponding aromatic dicarbaldehydes (**4**-**6**) [41]. Next, the Rap-Stoermer condensation of the intermediates with distinct phenacyl bromides in the presence of K_2CO_3 provided benzofurancarbaldehyde derivatives (**7**-**12**) in considerable to good yields [42]. Further, these benzofuran derivatives were subjected to the Hantzsch reaction, involving benzofuran aldehydes, active methylene ethyl/methyl acetoacetate, different 1,3-cyclohexadiones, and ammonium acetate (nitrogen donor) in the presence of glacial acetic acid gave the desired benzofuran-1, 4-dihydropyridine hybrids (**13**-**32**) in good yields (scheme 1a), while 1,4-dihydropyridine derivatives (**33**, **34**) were synthesised by the Hantzsch synthesis on benzaldehyde, ethyl acetoacetate and different 1,3 cyclohexadiones (scheme 1b).

Scheme 1. (a) Synthesis outline of benzofuran-1, 4-dihydropyridine hybrids. (b) Synthesis outline of 1, 4-dihydropyridine derivatives

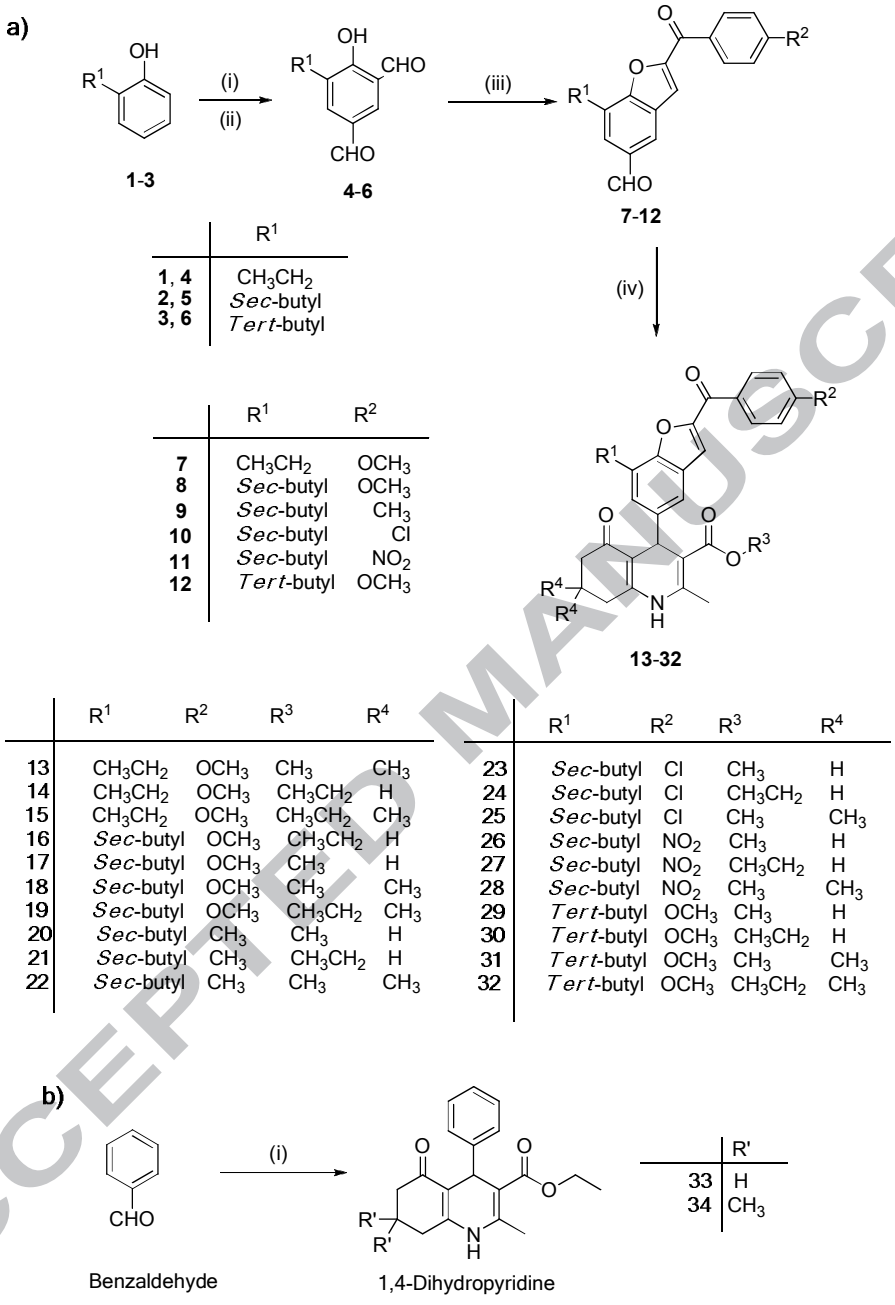

	R^1
1, 4	CH_3CH_2
2, 5	*Sec*-butyl
3, 6	*Tert*-butyl

	R^1	R^2
7	CH_3CH_2	OCH_3
8	*Sec*-butyl	OCH_3
9	*Sec*-butyl	CH_3
10	*Sec*-butyl	Cl
11	*Sec*-butyl	NO_2
12	*Tert*-butyl	OCH_3

	R^1	R^2	R^3	R^4
13	CH_3CH_2	OCH_3	CH_3	CH_3
14	CH_3CH_2	OCH_3	CH_3CH_2	H
15	CH_3CH_2	OCH_3	CH_3CH_2	CH_3
16	*Sec*-butyl	OCH_3	CH_3CH_2	H
17	*Sec*-butyl	OCH_3	CH_3	H
18	*Sec*-butyl	OCH_3	CH_3	CH_3
19	*Sec*-butyl	OCH_3	CH_3CH_2	CH_3
20	*Sec*-butyl	CH_3	CH_3	H
21	*Sec*-butyl	CH_3	CH_3CH_2	H
22	*Sec*-butyl	CH_3	CH_3	CH_3
23	*Sec*-butyl	Cl	CH_3	H
24	*Sec*-butyl	Cl	CH_3CH_2	H
25	*Sec*-butyl	Cl	CH_3	CH_3
26	*Sec*-butyl	NO_2	CH_3	H
27	*Sec*-butyl	NO_2	CH_3CH_2	H
28	*Sec*-butyl	NO_2	CH_3	CH_3
29	*Tert*-butyl	OCH_3	CH_3	H
30	*Tert*-butyl	OCH_3	CH_3CH_2	H
31	*Tert*-butyl	OCH_3	CH_3	CH_3
32	*Tert*-butyl	OCH_3	CH_3CH_2	CH_3

	R'
33	H
34	CH_3

Reagents and conditions (a):(i) HMTA, TFA, 120 °C, 4 h. (ii) aq H_2SO_4, 100 °C, 2 h (iii) Appropriate substituted phenacyl bromides, K_2CO_3/CH_3CN, 110 °C, 3 h, (iv) Ethyl/methyl acetoacetate, different 1,3-cyclohexadiones, NH_4OAc, AcOH, EtOH, reflux, 5 h. (b):(i) Ethyl acetoacetate, different 1,3-cyclohexadiones, NH_4OAc, AcOH, EtOH, reflux, 5 h.

2.2. ALP and mineralization activity in primary osteoblasts

Bone specific alkaline phosphatase (ALP) activity represents the proliferation of osteoblasts during bone formation. It is widely recognised biomarker to identify the lead candidate in a hit to lead optimization. We screened the racemic hybrids **13** to **32**, as well as their precursors (benzofurans) (**7** to **12**), and dihydropyridines (**33** and **34**) for stimulation of bone alkaline phosphatase (ALP) production in rat calvarial osteoblasts cells at different concentrations. Among the benzofuran and dihydropyridine parent compounds **7,8, 9,** and**33**showedsignificant activity at 10 nM and 100 pM which was comparatively less effective than the newly synthesized hybrid compounds. Compound **21** exhibited robust ALP activity at the lowest concentrations of 1 pM whereas, compound **12, 14** and **16** exhibited activity at 10 nM concentration compared to that of control. Among all screened compounds, eight compounds *i.e*, **7**, **8**, **9**, **12**, **14**, **16**, **21** and **33** were found to stimulate the ALP activity significantly (**Table 1**) and these compounds with their respective active concentration were selected for mineralization assay.

Table 1. Alkaline phosphatase (ALP) activity of all the screened compounds at different concentrations in calvarial osteoblast cells[a]

Compound	Control	1 pM	100 pM	10 nM	1 µM	100 µM
7	1.01±0.05	1.09±0.09	1.11±0.06	1.24±0.03*	1.03±0.05	0.29±0.01
8	1.03±0.12	1.35±0.01	**1.49±0.10***	**1.59±0.12****	1.21±0.12	0.58±0.08
9	1.01±0.07	1.23±0.07	1.16±0.07	**1.41±0.11****	**1.42±0.09****	0.30±0.01
10	1.06±0.07	0.98±0.06	0.78±0.05	0.96±0.06	0.77±0.05	0.26±0.01
11	1.06±0.06	1.04±0.11	0.66±0.06	0.73±0.08	1.08±0.09	0.31±0.01
12	1.21±0.07	1.33±0.10	1.50±0.16	1.70±0.19	1.26±0.05	0.59±0.02
13	1.11±0.09	1.26±0.25	0.73±0.08	1.19±0.14	1.20±0.15	0.18±0.01
14	1.04±0.10	1.32±0.19	1.49±0.15	**1.64±0.20***	**1.80±0.15****	0.41±0.04
15	1.12±0.28	1.24±0.20	1.45±0.23	1.65±0.28	1.72±0.26	0.50±0.16
16	1.03±0.07	0.94±0.09	0.99±0.07	**1.40±0.13***	**1.37±0.08***	0.25±0.01

17	1.02±0.09	1.37±0.08	1.34±0.13	1.09±0.12	1.34±0.13	0.37±0.03
18	1.06±0.09	0.97±0.09	0.64±0.07	1.14±0.12	1.26±0.09	0.29±0.03
19	1.06±0.11	1.08±0.04	0.82±0.05	1.30±0.13	1.13±0.12	0.51±0.11
20	1.07±0.04	0.99±0.07	1.12±0.05	1.17±0.07	0.84±0.05	0.25±0.01
21	1.0±0.03	**1.14±0.03***	**1.32±0.07*****	**1.19±0.03****	**1.16±0.02***	0.36±0.01
22	1.05±0.05	1.08±0.05	1.16±0.08	1.11±0.05	1.13±0.08	0.37±0.01
23	1.09±0.08	1.[39]±0.07	1.48±0.20	1.34±0.10	1.31±0.12	0.50±0.01
24	1.02±0.08	0.90±0.05	1.02±0.07	1.04±0.09	0.79±0.06	0.31±0.01
25	1.03±0.07	1.08±0.11	0.85±0.04	0.86±0.09	0.23±0.01	0.23±0.01
26	1.01±0.08	0.65±0.05	0.72±0.06	0.82±0.03	0.82±0.06	0.25±0.01
27	1.02±0.04	1.12±0.14	0.82±0.07	0.89±0.04	0.69±0.04	0.37±0.01
28	1.04±0.05	0.98±0.03	1.03±0.06	1.06±0.04	0.76±0.03	0.30±0.01
29	1.14±0.13	1.19±0.07	1.01±0.12	1.07±0.15	1.17±0.15	0.32±0.03
30	1.04±0.23	1.14±0.13	1.14±0.20	1.17±0.15	1.77±0.28	0.29±0.04
31	1.07±0.14	0.79±0.11	1.15±0.13	1.10±0.11	1.25±0.29	0.36±0.03
32	1.06±0.14	1.04±0.7	1.53±0.14	1.47±0.20	1.15±0.17	0.36±0.04
33	1.07±0.08	1.26±0.11	1.25±0.07	1.43±0.1*	1.44±0.10*	0.74±0.03
34	1.1±0.14	1.03±0.15	1.41±0.26	1.41±0.16	1.23±0.12	0.58±0.03

Data Values are expressed as Mean ± SEM. (n = 8).*p< 0.05, **p< 0.01 and ***p< 0.001 as compared with untreated cells taken as control only when ALP activity was higher.

Mineralization of bone is essential for bone hardness, strength and involves a well-organized process in which crystals of calcium phosphate is developed by bone-forming cells thatlay down in precise amounts within the bone matrix. In mineralization, we found that compounds **16** and **14** exhibited significantly higher mineralization at 10 nM and 1 μM concentrations respectively. Interestingly, compound **21** showed greater mineralizing ability at all concentrations ranging from 100 pM to 10 nM. Although, highest mineralizing effect of compound **21**as compared to other compounds were observed at 100 pM concentration **(Figure 2)**.This experimentnoticeably demonstrated that benzofuran-dihydropyridine hybrids were found to be more potent than their individuals.

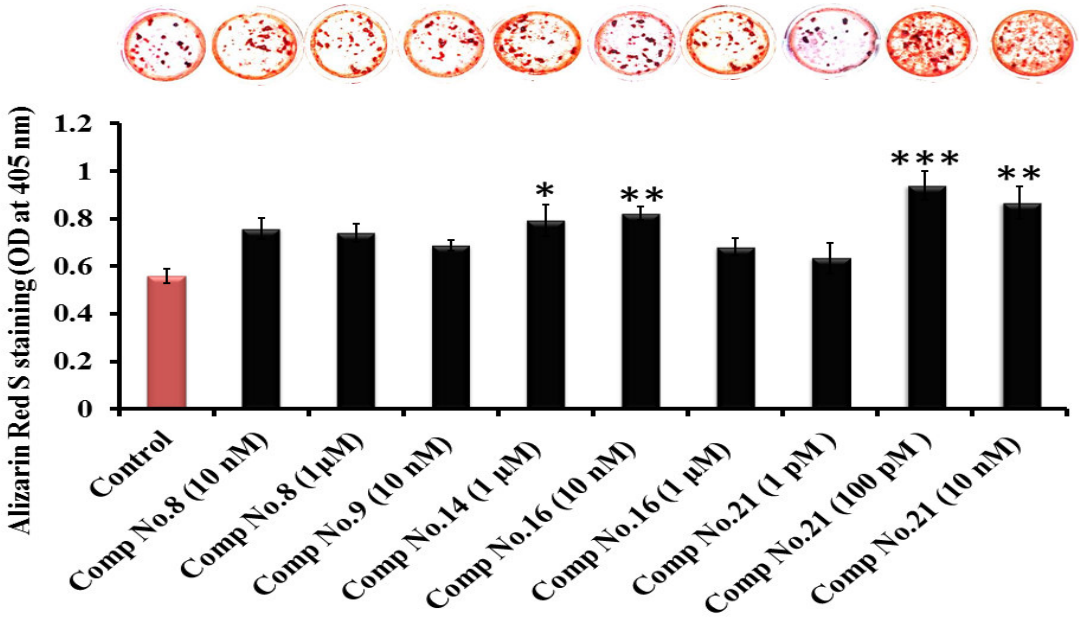

Figure 2 :- Mineralizing potential of compounds **8**, **9**, **14**, **16** and **21** as compared to the control (non-treated) cells in calvarial osteoblasts cells after 21 days of treatment in growth medium. Data represented as (n=8)Mean ± SEM. *p< 0.05, **p< 0.01 and ***p< 0.001 compared to controls.

2.3. Transcriptional analysis of osteogenic genes

We next assessed the effect of active compounds on osteogenic genes at the molecular level and the expression of alkaline phosphatase (*Alp*), osterix (*Osx*), collagen type-1 (*Col1*), runt-related transcription factor 2 (*Runx2*) and bone morphogenic protein-2 (*Bmp2*), regulating bone differentiation were assessed by qRT-PCR. 48-hour treatment revealed that the potent hybrids effectively increased the expression of osteogenic genes ranging from ~2.0 to ~5.5-folds over the control cells (**Figure 3**). At 10 nM concentration, compound **21** demonstrated significantly increased expressions of *Col1, Runx2 and Bmp2* genes that were in the order of 3.7, 3.4 and 3.1 folds respectively. However, 100 pM concentration of compound **21** exhibited maximum expression of all tested osteogenic genes; *Alp, Osx, Col1, Runx2 and Bmp2* osteogenic genes approximately 4.5, 3.7, 5.0, 3.9, and 4.5 folds respectively (**Figure**

3). This study shows that benzofuran-dihydropyridine hybrid compound **21** have potential to up regulate the expression of various key osteogenic genes.

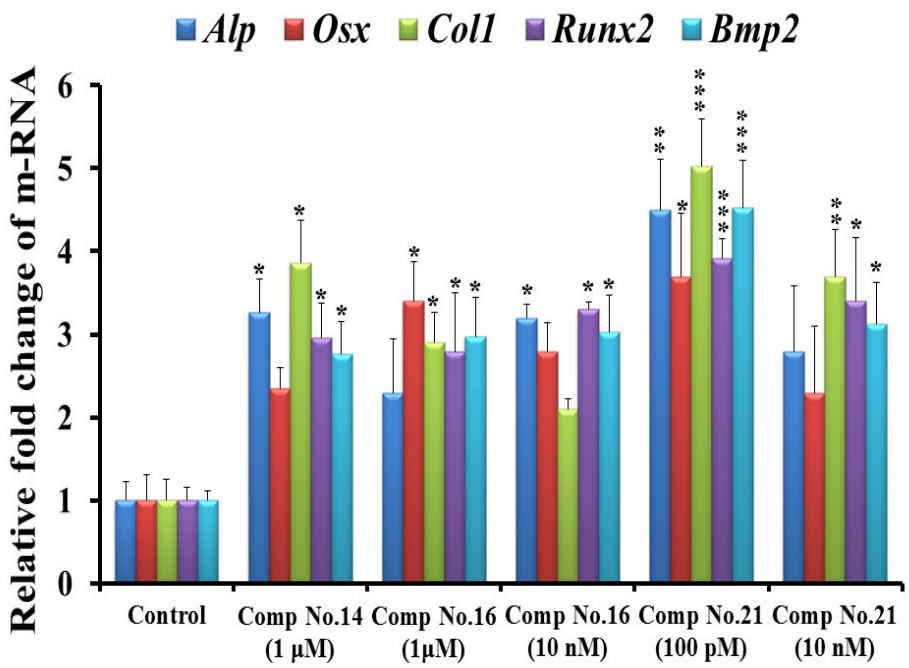

Figure 3 : Effect of compounds **9**, **14**, **16** and **21** on the expression of osteogenic genes (*Alp, Osx, Col1, Runx-2*and *Bmp2*) in calvarial osteoblasts as compared to control by qRT-PCR (n=5). Data represented as n=5 Mean ± SEM. *p< 0.05, **p< 0.01 and ***p< 0.001 compared to control.

2.4. BMP-2 elisa experiment

The synthesized compound **21**(100 pM) was evaluated by BMP2 Elisa assay. After treatment with the compound **21**, BMP2 expression was up-regulated (p<0.01) as compared to control group. From this study, it is evident that leads compound **21** increased expression of BMP2 in bone cells which plays an important role in osteoblast differentiation and bone regeneration (**Figure 4**).

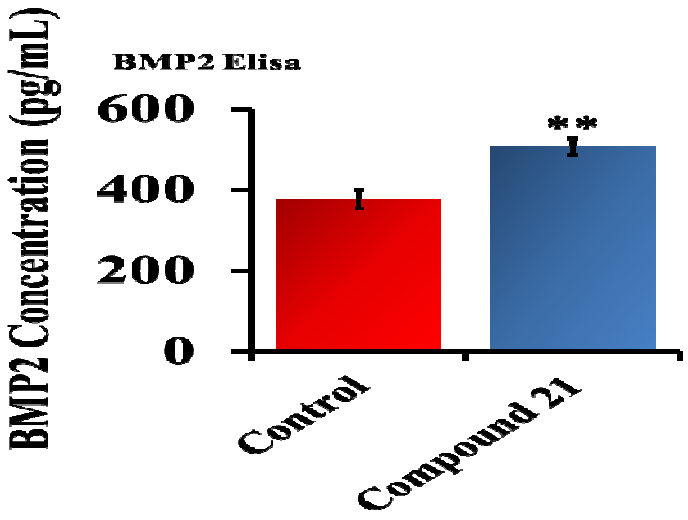

Figure 4: BMP2 elisa after 48 hours treatment. incalvarial osteoblasts as compared to control. Data represented as n=5 Mean ± SEM. ***p*< 0.01 compared to control.

2.5. Cell viability study

Preliminary cytotoxicity of the compound **21** by MTT assay was studied in calvarial osteoblasts cells. Data from the MTT assay suggested that compound **21** did not exhibit any toxicity to the cells at concentrations ranging from 1 pM to 1 µM compared to the control cells (**Figure 5**) corresponding to a significantly lower value of the ALP activity, compound **21** at 100 µM showed a cytotoxic effect on the osteoblast cells. From MTT studies we concluded that compound **21** was safe for osteoblasts cells and benzofuran-dihydropyridine hybrids could be novel agents for bone cells.The potential of compound **21** was also corroborated by its EC50 value (**Supporting Table S1**) and western blot analysis of osteogenic marker protein expression of RUNX2, BMP2 and COL1 (**SupportingFig. S2**).

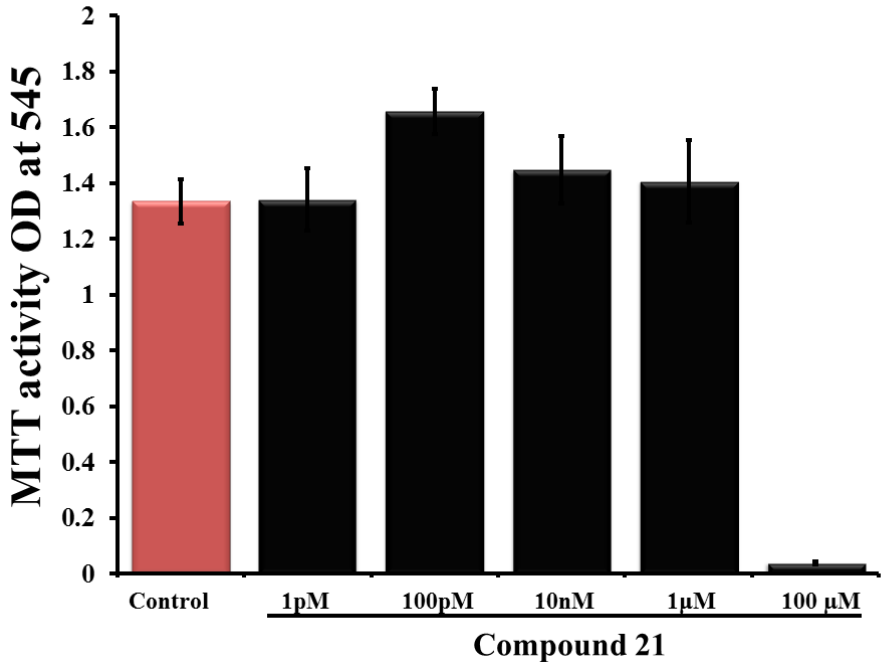

Figure 5 : Cells were cultured in differentiation medium and treated with various concentrations of the compound ranging from 1 pM to 100 µM for 24 h and cell viability assessed by MTT assay. Data represented as n=8 Mean ± SEM. compared to control.

*2.6. Subcutaneous injection of compound **21** for selecting best possible dose*

On the basis of promising in *vitro* potency and the expression of osteogenic genes compound **21**was selected for further in *in-vivo*assessment for osteogenesis. Compound **21** was administrated subcutaneously to skull region in 2 days old pups at doses of 0.1, 0.5, 1.0, and 5.0, 10.0 and 20 $mg.kg^{-1}day^{-1}$following three consecutive days. After 3 days injection pups were sacrificed and calvarial tissue was isolated for mRNA expression studies of osteogenic marker genes *Runx2* and *Bmp2*. Overall, on the basis of qRT-PCR data out of 6 doses of compound **21**, we selected 1.0, 5.0 and 10 $mg.kg^{-1}day^{-1}$ doses for *in-vivo* studies. On the basis of qRT-PCR data, we found that 1.0, 5.0, and 10 $mg.kg^{-1}day^{-1}$ doses showing good response but maximum responses of *Runx2* and *Bmp2* was shown by compound **21 at** 10 $mg.kg^{-1}day^{-1}$ dose. Further compound **21** had no significantly osteogenic responses and above10 $mg.kg^{-1}day^{-1}$ dose shows no dose-dependent response as represented in figure (**Figure6**).Therefore,

we took compound **21** and its active doses for further detailed in vivo evaluation in drill hole defect rat models.

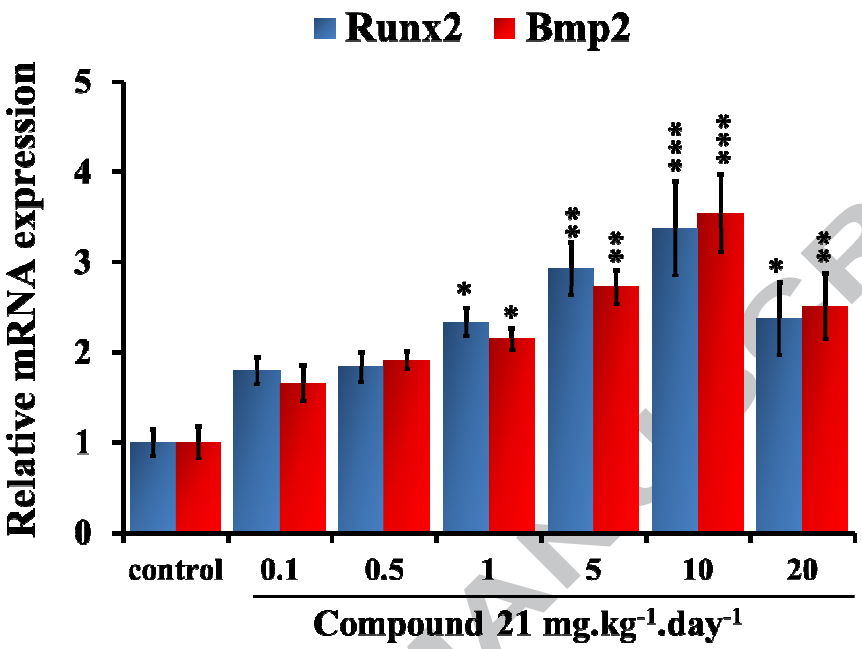

Figure 6 : ***Subcutaneous injection of compound 21 for selecting best possible doses.*** Data represented as n=5 Mean ± SEM. *p< 0.05, **p< 0.01 and ***p< 0.001 compared to control.

*2.7. Effect of the compound **21** in regeneration of bone at fracture site*

In order to quantitatively determine the bone healing process, we studied the effect of compound **21** on rapid fracture healing in the 0.8 mm drill hole defect fracture model in rats. After creation of 0.8 mm defect in femur bones of rodents we started treatment the next day with compound **21**at 10 mg.kg^{-1}day^{-1}dose for 14 days regularly. Representative images of rapid fracture healing at different doses in **Figure7a**, upper panel shows 3D images and lower panel shows 2D images. Data shows that compound **21** had higher bone volume/trabecular volume (BV/TV), trabecular thickness (Tb.Th), connection density (conn.D) and trabecular number (Tb.N) compared to the vehicle treated control group (**Figure 7b-7e**).These data indicated that compound **21**had significant effects that could restore bone-

microarchitecturewithpositive effects on bone formation parameters by expansion of new bone forming cells at the drill-hole injury site.

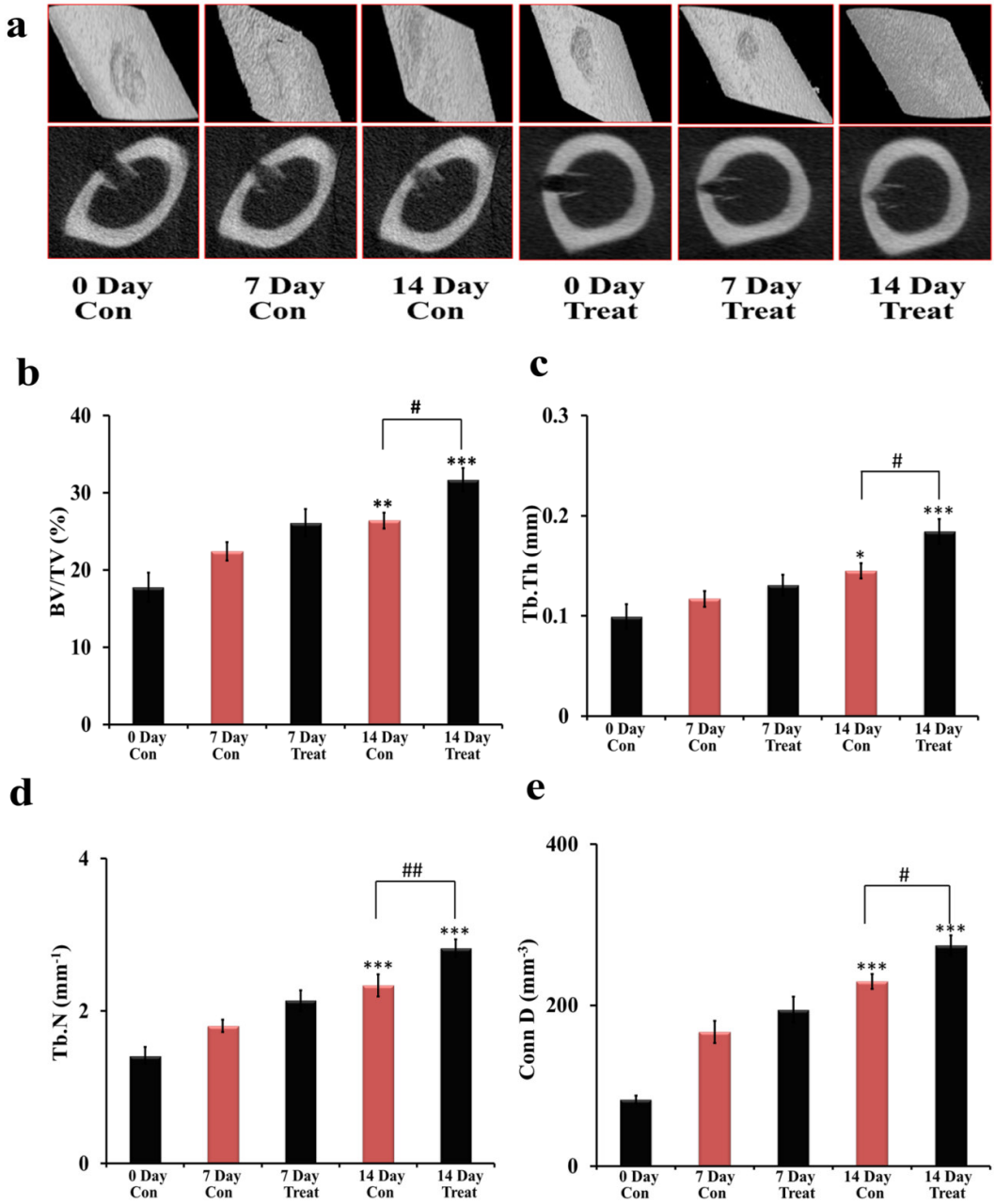

Figure 7 : Figure shows effect of compound **21** on drill hole bone defect. Figure **a** shows 3D and lower panelshows 2D images of 0.8 mm size defect, which was made at 2 cm above the knee joint of distal femur side. Figure c-f shows µ-CT analysis at defect site of the control and compound **21** treated groups. Lead compound **21** treatments had better micro architectural at defect site bt improving callus regeneration. **(b)** µ-CT analysis showing BV/TV (%), **(c)**Tb.Th (mm), **(d)**Tb.N (mm^{-1}), **(e)**Conn.D, (mm^{-3}). All values are expressed as

mean ± SEM (n = 6 rats/group); *p< 0.05; **p< 0.01; ***p< 0.001 compared to 0 day and $^{\#}p$ < 0.05, $^{\#\#}p$ < 0.01, $^{\#\#\#}p$ < 0.001 compared with 14 day of control group.

Data revealed that the lead compound increased the bone healing by enhancing callus regeneration at defect site. Histological changes with compound **21** showimproved callus regeneration. Enhanced callus regeneration at 50 µm size section of femur bone was observed (**Figure8a**), this finding was further validated by intensity of calcein labeling at defect site (**Figure8b**) and H&E staining of the callus (**Figure8c**). Analysis of mean intensity of calcein at the defect site by confocal microscope shows that treatment of compound **21** at a dose of 10 mg.kg^{-1}day^{-1} increased mineral deposition by enhancing callus regeneration in the defect site. Data of calcein labeling intensity showed that new bone formation was significantly improved ~40% (p< 0.01) at a dose of 10 mg.kg^{-1}day^{-1} treatment group compared to control (**Figure 8d**). Further, checked the qRT-PCR expression of *Bmp2* at defect site and found that compound **21** significantly increased the *Bmp2* expression (**Figure 8e**). From these studies, it conclude that compound **21** stimulates BMP2 production in bone forming cells that promotes bone formation at defect site. Benzofuran-dihydropyridine hybrid compound **21**has efficiency to upsurge fracture healing process as compare to their respective untreated control. Therefore compound **21** could be an attractive strategy to enhance fracture healing to shorten the healing period.

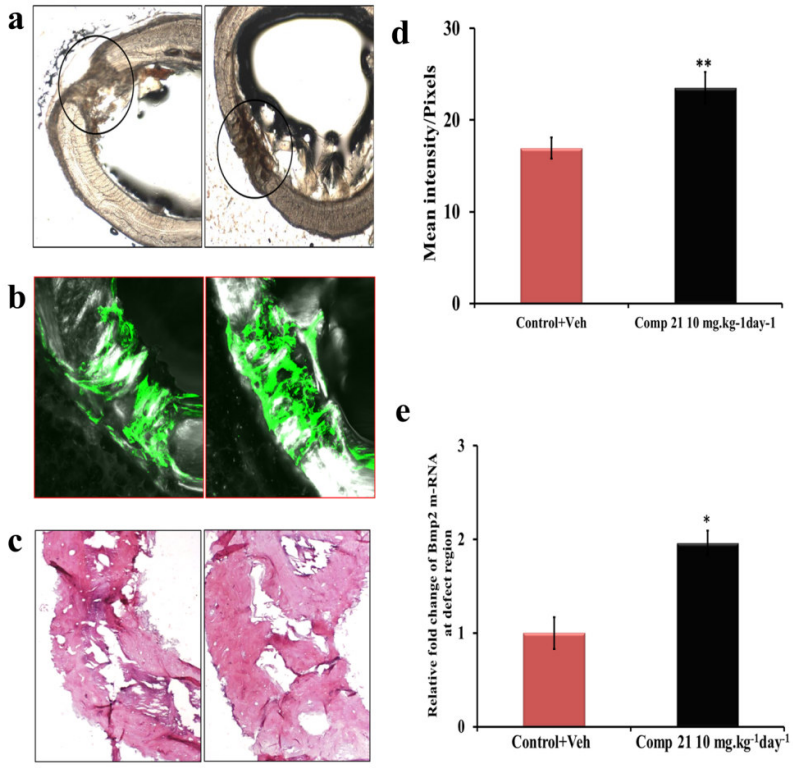

Figure 8 : Lead compound **21** treatments promote rapid fracture healing that was measured by calcein labeling intensity. **(a)** Representative images of bones with fracture healing of 50µm section sizes (4×). **(b)** Representative images of calcein labeling at defect site by confocal (20×) after two weeks of treatments. **(c)** Representative images of callus after H&E staining (10×). **(d)** Quantification of the mean intensity of calcein label per pixel. **(e)**Quantitative expression of Bmp2 by qRT-PCR at defect site in control and treated group. All values are expressed as mean ± SEM (n = 6 rats/group); **p*< 0.05; ***p*< 0.01; ****p*< 0.001 compared to control group.

*2.8. Effect of compound **21** on liver histomorphology for in vivo toxicity*

The safety assessment of the compound **21** was also carried out in liver tissue. Treatment with this compound orally for 14 days on rats was done and at the end of treatment livers from different groups of rats was collected and a histological analysis was performed using 5 µm thick sections. The liver histomorphology of the treated and untreated animals were similar and no morphological alterations were observed (**Figure9**).This study suggested that compound **21** to be safe and devoid of liver toxicity.

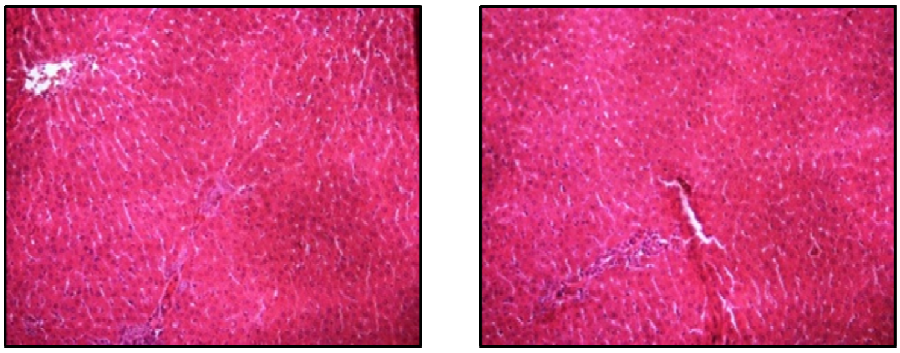

Control+Veh **Comp 21 10 mg.kg^{-1}day^{-1}**

Figure 9 : Sections of livers (20x) of SD rat after 12 weeks of lead compound **21** treatment with different doses (10 mg^{-1}kg^{-1}dayorally) and different control groups shows no significant changes in liver histology. Section observed from liver of 5 animals in each group

2.9. Structure-activity relationship (SAR) study

SAR was inferred from their activities in ALP and mineralization assay. For clear understanding of SAR, we have divided the hybrid molecules into northern hemisphere and southern hemisphere (**Figure 10**). In northern hemisphere, compounds containing methoxy and methyl substituted benzofuran compounds **7**, **8**, **9**, **14**, **16** and **21** were active for ALP and activity and compounds **14**, **16** and **21** were active for mineralization. At C-7 position *sec*-butyl group (**8**, **9**, **16** and **21**) and ethyl group (**7**, **14**) are more preferred than *tert*-butyl group (**29**, **30**, **31** and **32**), for activity. Compounds containing electron withdrawing groups like chlorine and nitro (**10**, **11**, **23**, **24**, **25**, **26**, **27** and **28**) were not favorable for the ALP activity. It is important to mention that though in the initial ALP activities benzofuran parent compounds **7**, **8**, **9** and **12** (non-dihydropyridine compound) showed significant activity, the presence of toxicophore (free aldehyde group) precluded us to proceed with this class and thus we proceeded to synthesize our designed hybrids that brought this free aldehyde into the reaction. In the case of southern hemisphere, compounds containing the unsubstitutedcyclohexanone and ethyl ester groups were found to be more potent (**14**, **16** and **21**) than compounds containing substituted cyclohexanone and methyl esters (**13**, **15**, **18**, **19**

and **22**). Interestingly, incorporation of the dihydropyridine moiety enhances activity in some cases (**14**, **16** and **21**).

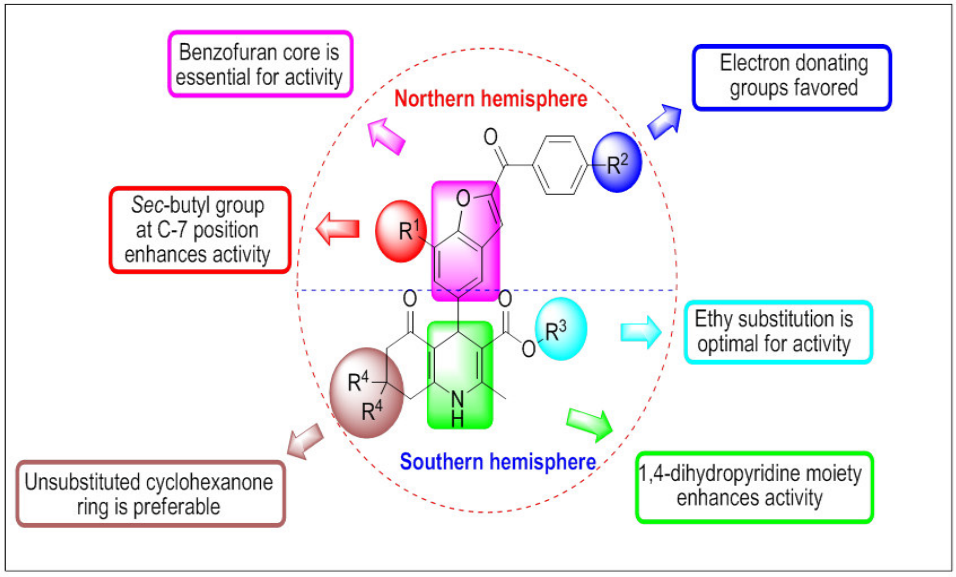

Figure 10:- SAR of the synthesized hybrids

3. Molecular modelling studies

Docking analysis was done to find the molecular interactions of active hybrid **21** on BMP-2. Due to the dimeric nature BMP-2 protein, dimeric structure of 3BK3 was used for interaction studies as functionality [43-45]. For the agonist crucial binding pocket was identified by the MetaPocket 2.0 as a putative binding site and was docked using AutoDock 4.2 [46].The binding pocket (Site-1) identified by the MetaPocket 2.0 tool was a deep seated cavity and was different from the binding sites of the 4 receptors **(Figure 11a, 11b)** as suggested by previous mutational studies [47]. Compound **21** is racemic and to get a preliminary insight we performed interactions studies for the major two isomers. For compound **21**(*S)* docking studies revealed a large cluster of 11 poses having lowest Kb (binding constant) of 6.96 µM and binding energy-7.05 kcal/mol. Compound **21**(*S*) at this pose shows hydrogen bond of

1.76 Å with amide group of Cys79, 2.07 Å and 2.67 Å with thiol group of Cys78, 3.24 Å forming hydrogen bond with amide of Cys47 (BMP2 of chain-A) and 2.03Å forming hydrogen bond with imidazole ring of His44 (BMP2 of chain-B) by its keto group of benzofuran ring (**Figure 11d**). For Compound **21**(*R*), large cluster of 18 poses with lowest Kb 10.58 μM and binding energy -6.79kcal/mol was observed at same binding pocket. At this pose, compound **21**(*R*) indicated possibility of hydrogen bond of 2.20Å with amide of Cys47 (BMP2 of chain-A) by its keto group of benzofuran ring; 1.92Å with imidazole ring of His44 and 2.26Å with carbonyl of Glu47 (BMP2 of chain-B) (**Figure 11e**).

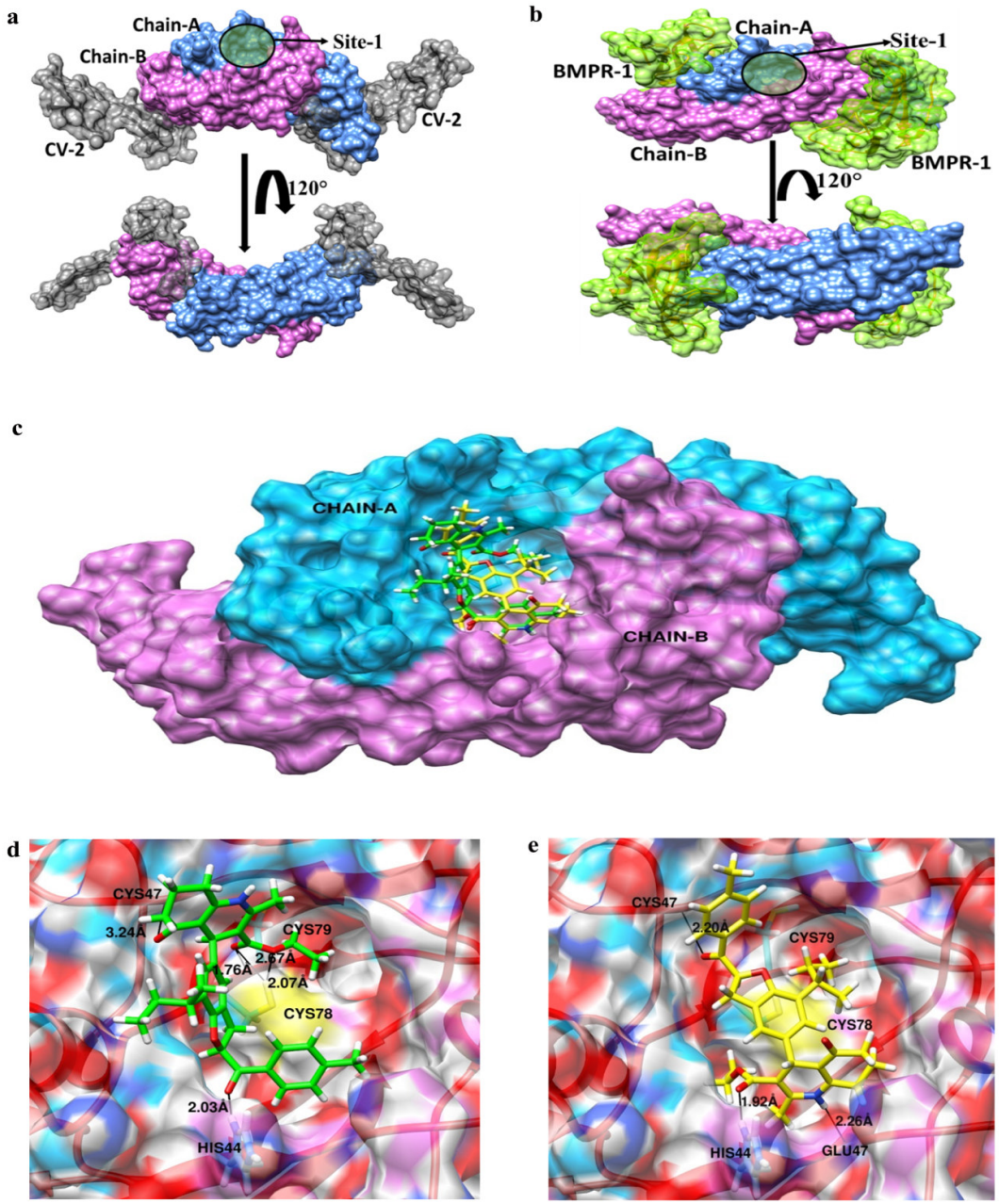

Figure 11: Figure 11a indicates the surface view model of dimer BMP2 along with the bound inhibitory CV-2 peptide (dark gray). The binding site predicted by MetaPocket 2.0 (Site-1) which was utilized for docking was different from this inhibitory peptide. Figure 11b indicated the dimer of BMP2 protein with BMPR-1 (green) having PDBid-2QJA. Interestingly it was observed that the interaction site of BMPR-1 to BMP2 is different from Site-1 predicted by MetaPocket 2.0. Figure 11c indicating slight variation in the interaction of compound **21**(S) w.r.t. compound **21**(R) at same binding pocket. Figure 11d and 11e indicating molecular interaction of compound **21**(S) (green) and compound **21**(R) (yellow) with BMP2 protein respectively.

Docking results **(Table 2)** and experimental results are in agreement with respect to the order of activity of compounds **21**, **16**, **14**, **9**, **8** and **DHP-1**. Binding studies indicated that presence of ethyl ester group of dihydropyridine ring imparts the compound highest activity due to hydrophobic interaction, followed by methyl ester group. Methyl substituent at *para*-position of benzene ring has lower Kb value than methoxy group as presence of methoxy group destabilizes hydrophobic interaction. Interaction studies do indicate the importance of backbone amide (Cys47 and Cys79) and carbonyl groups (Glu47) that are completely buried in the hydrophobic contact region as major binding determinants. Also, it has been observed that presence of keto group of benzofuran ring imparts more activity to agonist possibly by forming strong hydrogen bonds. Furthermore, molecular modelling studies that were performed to gain insight into the binding mode revealed that both benzofuran and dihydropyridine moieties are essential to show similar binding interactions to fit into the binding site of BMP2 lead compound. Computational studies have indicated that this deep seated cavity in the dimerfunctions as binding site for our lead compounds. The increased level of BMP-2 in presence of our lead compounds(observed by Western blot assay) possibly indicate that our lead compounds may stabilize the BMP-2 dimer. This stabilized dimer, as computational studies suggest may still be free for interaction with BMPR-1 and BMPR-2 simultaneously and form hetero-tetrameric complex [48-51]. Molecular modelling studies not only revealed the structural insights of the potent hybrid, but also inspired us to synthesize enantiomerically pure compounds, which will be our future priority.

Table 2.Computational data docking results: Binding energy values of active compounds

Name of Compound	**Binding Energy** (Kcal/mol)	**Kb Value** (μM)	**Number of poses in cluster**
21(*R*)	-6.79	10.58	18
21(*S*)	-7.05	6.78	11
16(*R*)	-5.89	48.16	16
16(*S*)	-6.93	8.31	14

14(*R*)	-6.35	21.84	13
14(*S*)	-6.36	21.65	13
9	-5.50	92.57	25
8	-5.71	65.38	28
33(*R*)	-5.52	89.54	36
33(*S*)	-5.46	98.95	13

Legends: The table summarizes the binding energies of various compounds along with BMP-2 dimer along with the number of poses observed in the cluster.

4. Conclusion

In our studies, compound **21** was found to significantly stimulate BMP2 and osteoblast differentiation from a series of structurally similar compounds of benzofuran-dihydropyridine hybrids. Compound **21** was found to increase alkaline phosphatase activity, which is the essential step in the process of evaluation of osteogenic compounds. It also enhanced osteoblasts by improve mineralization activity in extra cellular matrix.It also enhanced the mRNA expression of osteogenic markers genes expression of RUNX2, BMP2 and COL1 that are the hallmark in process of new bone formation acts as a factor promoting osteoblast function. BMP2 plays an important role in fracture healing by stimulation and differentiation of mesenchymal progenitor cells in osteoblasts at fracture site. In this direction compound **21** increased BMP2 formations. Further, we studied the in-vivo efficacy of compound **21** in a drill-hole fracture (defect) model for rapid bone healing process in femoral bone. Data showed that compound 21 triggers the regeneration and healing properties in bone compared to the vehicle treated group. From by µCT analysis data, it is can be verified that oral administration of lead compound **21**mitigatesmicro-architectural loss of bone tissue by increasing trabecular number and bone volume that indicate recovery of trabecular bone micro-architecture with better connectivity at 10 $mg.kg^{-1}day^{-1}$ dose in drill hole rats. These in-vitro and in-vivo results suggested that the compound **21** stimulate new bone formation at fracture site by increasing BMP2 production that leads to improve in structure of bone

trabecular bone microarchitecture at drill hole site. Through computational studies, we concluded that our lead compound possible bind to a deep seated cavity in dimeric conformation of BMP2 protein and this site stabilize the BMP2 dimer, which further induce osteogenic responses. Due to the absence of in-vitro and in-vivo toxicity, compound **21** could be developed as alternative for shorten the healing period. Lastly, this compound provides a scaffold and platform for the development of new bone forming agents against bone related disorders.

5. Experimental Section

5.1. General Procedure: All reagents were commercial available and were used without further purification. Chromatography was carried on silica gel (100-200 and 230-400 mesh). All reactions were monitored by thin-layer chromatography (TLC), silica gel plates with fluorescence F254 were used. Melting points were taken in open capillaries on Stuart-SMP30 melting point apparatus and are presented uncorrected. Infrared spectra were recorded on a Perkin-Elmer FT-IR RXI spectrophotometer. ^{1}H NMR and ^{13}C NMR spectra were recorded using BrukerSupercon Magnet DRX-300 spectrometer (operating at 300 and 400 MHz for ^{1}H and 75 and 100 MHz for ^{13}C) using $CDCl_3$ and DMSO-d_6 as solvent whereas tetramethylsilane (TMS) taken as internal standard. Chemical shifts were reported in parts per million and multiplicity (s = singlet, brs = broad singlet, d = doublet, brd = broad doublet, dd = double doublet, t = triplet, q = quartet, m = multiplet). Electro spray ionization mass spectra (ESI-MS) were recorded on Thermo Lcq Advantage Max-IT. High resolution mass spectra (HRMS) were recorded on 6520 Agilent Q Tof LC MS/MS (Accurate mass).High performance liquid chromatography analyses for checking purity of targeted compounds were performed on Shimadzu SCL 20 Avp, which was equipped with an Shimadzu SIL-HTC autosampler on a Agilent Zorbax C18 column (100 mm x 4.6 mm, having particle size 5 µm).

Isocratic elution was carried out using mobile phase consisting of 10 mM ammonium acetate (containing pH 5.0) and acetonitrile at 10: 90 % (v/v). All targeted final compounds were found to have >95% purity by HPLC.

5.2. Typical method for the preparation of Compounds 1 to 3

Starting materials (**1**-**3**) were commercially available and were used without further purification.

5.3. Typical method for the preparation of Compounds 4 to 6

Synthesis of dicarbaldehyde substrates (Compounds **4** to **6)** were achieved by our previously reported protocol [33].

5-Ethyl-4-hydroxyisophthalaldehyde (**4**)

White solid, yield: 69%; mp: 173-174 °C; 1H NMR (400 MHz, $CDCl_3$) δ: 11.85 (s, 1H), 9.98 (s, 1H), 9.91 (s, 1H), 7.97-7.95 (m, 2H), 2.78-2.72 (m, 2H), 1.26 (t, 3H, J = 7.5 Hz); IR (neat): 3259, 2870, 1700, 1628, 1013 cm-1; ESI-MS: m/z: 179 (M+H)+; HRMS m/z:calcd for $C_{10}H_{10}O_3$ (M+H) + 179.0708, found 179.0711.

5-Sec-butyl-4-hydroxybenzene-1,3-dicarbaldehyde (**5**)

Oily; Yield 55%; ^{1}H NMR (400 MHz, $CDCl_3$) δ: 11.99 (s, 1H), 10.05 (s, 1H), 9.97 (s, 1H), 8.09 (brs, 1H), 8.00 (brs, 1H), 3.27−3.10 (m, 1H), 1.74−1.57 (m, 2H), 1.26 (d, 3H, *J* = 7.0 Hz), 0.86 (t, 3H, *J* = 7.3Hz); ^{13}C NMR (75 MHz, $CDCl_3$); 190.1, 163.3, 156.5, 155.8, 149.0, 137.5, 133.0, 131.9, 129.9, 118.9, 118.0, 53.2, 33.4, 29.6, 20.4, 12.0; IR (neat): 3267, 2862, 1709, 1622, 1018 cm^{-1}. ESI-MS *m/z*: 207 $(M + H)^+$; HRMS *m/z:*calcd for $C_{12}H_{14}O_3$ $(M+H)^+$ 207.1021, found 207.1016.

5-Tert-butyl-4-hydroxyisophthalaldehyde (**6**)

Oily; Yield: 65%; ^{1}H NMR (400 MHz, $CDCl_3$) δ: 12.39 (s, 1H), 9.99 (s, 1H), 9.93 (s, 1H), 8.07 (brs, 1H), 7.99 (brs, 1H), 1.46 (s, 9H); ^{13}C NMR (100 MHz, $CDCl_3$); 196.4, 190.0, 166.1, 140.0, 135.4, 133.9, 128.6, 120.4, 35.2, 29.1; IR (neat): 3252, 2865, 1703, 1626, 1013

cm^{-1}; ESI-MS *m/z*: 207 $(M+H)^+$; HRMS *m/z:*calcd for $C_{12}H_{14}O_3$ $(M+H)^+$ 207.1021, found 207.1018.

5.4 Typical method for the preparation of compounds 7 to 12

General synthetic procedure for preparation of 7-(sec-butyl)-2-(4-methoxybenzoyl) benzofuran-5-carbaldehyde (**8**)

To a mixture of 5-(sec-butyl)-4-hydroxyisophthalaldehyde (**5**) (1.0 mmol), 4-methoxyphenacylbromide (1.2 mmol) and K_2CO_3 (0.6 mmol), acetonitrile (20 mL) was added. The reaction mixture was refluxed for 3h. After completion of the reaction, K_2CO_3 was removed in a sintered funnel, and the filtrate was concentrated under vacuum and subjected to column chromatography with ethylacetate-hexane (15:85, v/v) to give pure compound **8** as a white solid.

The compounds (**7**-**12**) were prepared in a way similar to the procedure described above.

7-(Sec-butyl)-2-(4-methoxybenzoyl) benzofuran-5-carbaldehyde (**8**)

White solid, yield: 68 %; mp: 74-75 °C; ^{1}H NMR (400 MHz, $CDCl_3$) δ: 10.07 (s, 1H), 8.14 (d, 2H, *J* = 8.9 Hz), 8.09 (d, 1H, *J* = 1.6 Hz), 7.87 (d, 1H, *J* = 1.2 Hz), 7.63 (s, 1H), 7.03 (d, 2H, *J* = 8.9 Hz), 3.92 (s,3H), 3.39-3.30 (m, 1H), 1.89-1.78 (m, 2H), 1.43 (d, 3H, *J* = 6.9 Hz), 0.89 (t, 3H, *J* = 7.3 Hz); ^{13}C NMR (100 MHz, $CDCl_3$) : 191.7, 182.2, 163.9, 157.4, 154.2, 133.6, 133.4, 132.1, 129.5, 127.3, 125.4, 124.8, 115.5, 114.0, 55.6, 35.9, 29.7, 20.3, 12.2; IR (KBr): 3050, 1680, 1654, 1651, 1210, 768 cm^{-1}; ESI-MS *m/z*: 337 $(M+H)^+$; HRMS *m/z:*calcd for $C_{21}H_{20}O_4$ $(M+H)^+$ 337.1440, found 337.1434.

7-(Sec-butyl)-2-(4-methylbenzoyl)benzofuran-5-carbaldehyde (**9**)

Oily; yield: 70 %; ^{1}H NMR (400 MHz, $CDCl_3$) δ: 10.07 (s, 1H), 8.09 (d, 1H, *J* = 1.5 Hz), 8.00 (d, 2H, *J* = 8.2 Hz), 7.87 (d, 1H, *J* = 1.2 Hz), 7.63 (s, 1H), 7.36 (d, 2H, *J* = 8.0 Hz), 3.38-3.32 (m,1H), 2.47 (s, 3H), 1.88-1.80 (m, 2H), 1.43 (d, 3H, *J* = 7.0 Hz), 0.89 (t, 3H, *J* = 7.4 Hz); ^{13}C NMR (100 MHz, $CDCl_3$) : 191.6, 183.5, 157.5, 153.9, 144.3, 134.3, 133.8, 133.4,

129.8, 129.4, 127.3, 125.6, 124.9, 35.9, 29.7, 21.8, 20.3, 12.3; IR (KBr): 3043, 1684, 1659, 1629, 1204, 755 cm^{-1}; ESI-MS *m/z*: 321 $(M+H)^+$; HRMS *m/z:*calcd for $C_{21}H_{20}O_3$ $(M+H)^+$ 321.1491, found 321.1500.

7-(Sec-butyl)-2-(4-chlorobenzoyl)benzofuran-5-carbaldehyde (**10**)

Oily; yield: 70 %; ^1H NMR (400 MHz, $CDCl_3$) δ: 10.07 (s, 1H), 8.10 (d, 1H, *J* = 1.5 Hz), 8.05 (d, 2H, *J* = 8.6 Hz), 7.89 (d, 1H, *J* = 1.2 Hz), 7.66 (s, 1H), 7.54 (d, 2H, *J* = 8.6 Hz), 3.36-3.30 (m,1H), 1.88-1.78 (m, 2H), 1.43 (d, 3H, *J* = 7.0 Hz), 0.89 (t, 3H, *J* = 7.3 Hz); ^{13}C NMR (100 MHz, $CDCl_3$) : 182.6, 171.9, 157.4, 153.3, 139.9, 135.2, 133.0, 131.1, 129.1, 127.7, 127.0, 125.8, 124.4, 116.7, 36.1, 29.8, 20.4, 12.3; IR (KBr): 3020, 1691, 1646, 1600, 1217, 777 cm^{-1}; ESI-MS *m/z*: 341 $(M+H)^+$; HRMS *m/z:*calcd for $C_{20}H_{17}ClO_3$ $(M+H)^+$ 341.0944, found 341.0939.

7-(Sec-butyl)-2-(4-nitrobenzoyl)benzofuran-5-carbaldehyde (**11**)

White solid, yield: 80%; mp: 117-118 °C; ^1H NMR (400 MHz, $CDCl_3$) δ: 10.09 (s, 1H), 8.41 (d, 2H, *J* = 8.9 Hz), 8.24 (d, 2H, *J* = 8.9 Hz), 8.13 (d, 1H, *J* = 1.5 Hz), 7.92 (d, 1H, *J* = 1.2 Hz), 7.73 (s, 1H), 3.35-3.30 (m,1H), 1.87-1.81 (m, 2H), 1.43 (d, 3H, *J* = 7.0 Hz), 0.89 (t, 3H, *J* = 7.4 Hz); ^{13}C NMR (100 MHz, $CDCl_3$) : 191.4, 182.0, 157.8, 152.9, 150.4, 141.7, 134.0, 133.8, 130.6, 127.1, 126.5, 125.2, 123.9, 117.5, 36.0, 29.7, 20.3, 12.3;IR (KBr): 3030, 1670, 1665, 1615, 1537, 1229, 768 cm^{-1}; ESI-MS *m/z*: 352 $(M+H)^+$; HRMS *m/z:*calcd for $C_{20}H_{17}NO_5$ $(M+H)^+$ 352.1185, found 352.1184.

5.5 Typical method for the preparation of compounds 13 to 32

General synthetic procedure for preparation of *Methyl-4-(7-ethyl-2-(4-methoxybenzoyl)benzofuran-5-yl)-2,7,7-trimethyl-5-oxo-1,4,5,6,7,8-hexahydroquinoline-3-carboxylate* (**13**)

To a solution of 7-ethyl-2-(4-methoxybenzoyl)benzofuran-5-carbaldehyde (1.0 mmol) (**7**) in 5 mL ethanol were added methyl acetoacetate (1.0 mmol), 1,3-cyclohexadione (1.0 mmol),

ammonium acetate (3.0 mmol), and 5 mL glacial acetic acid. The reaction mixture was continued under reflux condition for 8 h. After completion of reaction (monitored by TLC), the reaction mixture was cooled to room temperature. The solid thus obtained was filtered and subjected to column chromatography with ethylacetate-hexane (40:60, v/v) furnishing compound **13** as a white solid in good yield.

Methyl-4-(7-ethyl-2-(4-methoxybenzoyl)benzofuran-5-yl)-2,7,7-trimethyl-5-oxo-1,4,5,6,7,8-hexahydroquinoline-3-carboxylate (**13**)

White solid, yield: 80%; mp: 129-130 °C;^{1}H NMR (400 MHz, DMSO-d_6) δ: 9.13 (s, 1H), 8.03 (d, 2H, *J* = 8.9 Hz), 7.68 (s, 1H), 7.36 (d, 1H, *J* = 1.4 Hz), 7.23 (s, 1H), 7.11 (d, 2H, *J* = 8.9 Hz), 4.98 (s, 1H), 3.87 (s, 3H), 3.53 (s, 3H), 2.91-2.79 (m, 2H), 2.50-2.42 (m, 5H), 2.31-1.96 (m, 2H), 1.26 (t, 3H, *J* = 7.5 Hz), 1.01 (s, 3H), 0.84 (s, 3H); ^{13}C NMR (100 MHz, $CDCl_3$): 195.8, 183.1, 168.1, 163.6, 153.6, 152.5, 148.9, 144.2, 143.5, 132.1, 130.1, 128.1, 127.9, 126.5, 119.4, 116.7, 113.9, 112.1, 105.9, 55.6, 51.1, 40.9, 36.5, 32.7, 29.6, 27.0, 23.0, 19.4, 14.2; IR (KBr): 3252, 3069, 1491, 1217, 1683 cm^{-1}; ESI-MS: m/z: 528 $(M+H)^+$; HRMS *m/z*calcd for $C_{32}H_{33}NO_6$ $(M+H)^+$ 528.2386, found 528.2385.

Ethyl-4-(7-ethyl-2-(4-methoxybenzoyl)benzofuran-5-yl)-2-methyl-5-oxo-1,4,5,6,7,8-hexa hydroquinoline-3-carboxylate (**14**)

White solid, yield: 78%; mp: 210-211 °C;^{1}H NMR (500 MHz, DMSO-d_6) δ: 9.16 (s, 1H), 8.03 (d, 2H, *J* = 8.9 Hz), 7.68 (s, 1H), 7.36 (s, 1H), 7.36 (s, 1H), 7.26 (d, 1H, *J* = 1.4 Hz), 7.11 (d, 2H, *J* = 8.9 Hz), 5.00 (s, 1H), 4.00-3.96 (m, 2H), 3.87 (s, 3H), 2.91-2.82 (m, 2H), 2.51-2.49 (m, 2H), 2.30-2.15 (m, 2H), 1.93-1.74 (m, 2H), 1.29 (t, 3H, *J* = 7.5 Hz), 1.13 (t, 3H, *J* = 7.0 Hz); ^{13}C NMR (100 MHz, $CDCl_3$) : 196.1, 183.1, 167.6, 163.7, 153.7, 152.5, 150.7, 143.9, 143.8, 132.1, 130.1, 128.4, 127.9, 126.6, 119.6, 116.5, 113.9, 113.4, 106.2, 59.9, 55.6, 37.1, 36.6, 27.4, 23.1, 21.1, 19.3, 14.4, 14.1; IR (KBr): 3350, 3020, 1670, 1469,

1215 cm^{-1}; ESI-MS *m/z*: 514 $(M+H)^+$; HRMS *m/z*calcd for $C_{31}H_{31}NO_6$ $(M+H)^+$ 514.2230, found 514.2226.

Ethyl-4-(7-ethyl-2-(4-methoxybenzoyl)benzofuran-5-yl)-2,7,7-trimethyl-5-oxo-1,4,5,6,7,8-hexahydroquinoline-3-carboxylate (**15**)

White solid, yield: 80%; mp: 127-128 °C; ^{1}H NMR (400 MHz, DMSO-d_6) δ: 9.09 (s, 1H), 8.03 (d, 2H, *J* = 8.8 Hz), 7.69 (s, 1H), 7.38 (d, 1H, *J* = 1.5 Hz), 7.24 (s, 1H), 7.11 (d, 2H, *J* = 8.8 Hz), 4.95 (s, 1H), 4.00-3.95 (m, 2H), 3.87 (s, 3H), 2.94-2.79 (m, 2H), 2.50-2.30 (m, 5H), 2.20-1.95 (m, 2H), 1.26 (t, 3H, *J* = 7.5 Hz), 1.14 (t, 3H, *J* = 7.0 Hz), 1.01 (s, 3H), 0.85 (s, 3H); ^{13}C NMR (100 MHz, $CDCl_3$): 198.7, 196.5, 195.6, 183.0, 167.6, 163.6, 153.7, 152.6, 148.2, 143.6, 143.5, 132.1, 130.2, 128.2, 127.9, 126.6, 119.6, 116.5, 113.9, 112.5, 106.5, 59.9, 55.6, 50.8, 41.2, 36.7, 32.8, 29.6, 27.1, 23.1, 19.6, 14.4, 14.2; IR (KBr): 3330, 3020, 1639, 1480, 1243 cm^{-1}; ESI-MS *m/z*: 542 $(M+H)^+$; HRMS *m/z*calcd for $C_{33}H_{35}NO_6$ $(M+H)^+$542.2543, found 542.2549.

Ethyl-4-(7-(sec-butyl)-2-(4-methoxybenzoyl)benzofuran-5-yl)-2-methyl-5-oxo-1,4,5,6,7,8-hexahydroquinoline-3-carboxylate (**16**)

White solid, yield: 76%; mp: 198-199 °C;^{1}H NMR (500 MHz, DMSO-d_6) δ: 9.16 (s, 1H), 8.03 (d, 2H, *J* = 8.8 Hz), 7.68 (s, 1H), 7.33 (d, 1H, *J* = 1.6 Hz), 7.26 (s, 1H), 7.11 (d, 2H, *J* = 8.8 Hz), 5.00 (s, 1H), 4.00-3.96 (m, 2H), 3.87 (s, 3H), 3.12-3.05 (m, 1H), 2.51-2.49 (m, 2H), 2.29 (s, 3H), 2.22-2.15 (m, 2H), 1.93-1.69 (m, 4H), 1.31 (t, 3H, *J* = 6.4 Hz), 1.13 (t, 3H, *J* = 7.1 Hz), 0.80 (t, 3H, *J* = 7.3 Hz); ^{13}C NMR (100 MHz, $CDCl_3$): 196.0, 183.0, 167.6, 163.6, 153.4, 153.3, 152.5, 150.5, 143.9, 143.8, 132.1, 131.2, 131.1, 130.0, 127.4, 127.1, 126.9, 126.8, 119.3, 116.4, 113.9, 113.5, 106.2, 59.9, 55.6, 37.1, 36.5, 36.1, 29.8, 29.6, 27.4, 21.2, 20.4, 19.3, 14.4, 12.4; IR (KBr): 3390, 3019, 1643, 1467, 1259 cm^{-1}; ESI-MS *m/z*: 542 $(M+H)^+$; HRMS *m/z*calcd for $C_{33}H_{35}NO_6$ $(M+H)^+$ 542.2543, found 542.2548.

Methyl-4-(7-(sec-butyl)-2-(4-methoxybenzoyl)benzofuran-5-yl)-2-methyl-5-oxo-1,4,5,6,7,8-hexahydroquinoline-3-carboxylate (**17**)

White solid, yield: 78%; mp: 190-191 °C;^{1}H NMR (400 MHz, DMSO-d_6) δ: 9.19 (s, 1H), 8.02 (d, 2H, J = 7.7 Hz), 7.67 (s, 1H), 7.32 (s, 1H), 7.25 (s, 1H), 7.11 (d, 2H, J = 7.7 Hz), 5.01 (s, 1H), 3.87 (s, 3H), 3.53 (s, 3H), 3.16-3.07 (m, 1H), 2.49 (brs, 2H), 2.29 (s, 3H), 2.19 (brs, 2H), 1.73-1.70 (m, 4H), 1.32 (d, 3H, J = 7.0 Hz), 0.79 (brs, 3H); ^{13}C NMR (100 MHz, $CDCl_3$): 196.1, 183.0, 168.1, 163.6, 153.3, 152.5, 150.9, 144.3, 143.8, 132.1, 131.2, 130.0, 127.3, 126.8, 119.1, 116.4, 113.9, 113.3, 105.8, 55.6, 51.1, 37.1, 36.5, 36.3, 35.8, 29.7, 27.3, 21.1, 20.4, 19.2, 12.3, 12.1; IR (KBr): 3264, 3089, 1686, 1440, 1228 cm^{-1}; ESI-MS *m/z*: 528 $(M+H)^+$;HRMS *m/z*calcd for $C_{32}H_{33}NO_6$ $(M+H)^+$ 528.2386, found 528.2385.

Methyl-4-(7-(sec-butyl)-2-(4-methoxybenzoyl)benzofuran-5-yl)-2,7,7-trimethyl-5-oxo-1,4,5,6,7,8-hexahydroquinoline-3-carboxylate (**18**)

White solid, yield: 80%; mp: 138-139 °C;^{1}H NMR (500 MHz, DMSO-d_6) δ: 9.14 (s, 1H), 8.03 (d, 2H, J = 8.0 Hz), 7.68 (s, 1H), 7.34 (s, 1H), 7.24 (s, 1H), 7.11 (d, 2H, J = 8.1 Hz), 4.98 (s, 1H), 3.87 (s, 3H), 3.53 (s, 3H), 3.10-3.06 (m, 1H), 2.50-2.26 (m, 5H), 2.21-1.96 (m, 2H), 1.68 (t, 2H, J = 6.6 Hz), 1.29 (d, 3H, J = 6.8 Hz), 1.01 (s, 3H), 0.82 (s, 3H), 0.77 (brs, 3H); ^{13}C NMR (100 MHz, $CDCl_3$) : 195.8, 183.0, 168.0, 163.6, 153.4, 153.3, 152.4, 148.9, 144.4, 144.3, 143.5, 143.4, 132.1, 131.4, 130.1, 127.0, 126.7, 119.1, 116.5, 113.9, 112.1, 105.8, 55.6, 51.1, 40.9, 36.4, 32.6, 29.7, 26.9, 20.5, 20.4, 19.3, 12.3; IR (KBr): 3310, 3020, 1635, 1471, 1223 cm^{-1}; ESI-MS *m/z*: 556 $(M+H)^+$; HRMS *m/z*calcd for $C_{34}H_{37}NO_6$ $(M+H)^+$556.2699, found 556.2693.

Ethyl-4-(7-(sec-butyl)-2-(4-methoxybenzoyl)benzofuran-5-yl)-2,7,7-trimethyl-5-oxo-1,4,5,6, 7,8-hexahydroquinoline-3-carboxylate (**19**)

White solid, yield: 78%; mp: 135-136 °C;^{1}H NMR (400 MHz, DMSO-d_6) δ: 9.11 (s, 1H), 8.03 (d, 2H, J = 8.8 Hz), 7.69 (s, 1H), 7.36 (s, 1H), 7.24 (s, 1H), 7.11 (d, 2H, J = 8.8 Hz),

4.97 (s, 1H), 4.00-3.87 (m, 2H), 3.31 (s, 3H), 3.12-3.05 (m, 1H), 2.47-2.27 (m, 5H), 2.20-1.95 (m, 2H), 1.74-1.67 (m, 2H), 1.30-1.27 (m, 3H), 1.14 (t, 3H, *J* = 8.8 Hz), 1.01 (s, 3H), 0.83 (s, 3H), 0.77 (t, 3H, *J* = 7.3 Hz) ; ^{13}C NMR (100 MHz, $CDCl_3$) : 195.7, 183.0, 167.6, 163.6, 153.4, 153.3, 152.5, 148.7, 143.9, 143.6, 132.1, 131.4, 130.1, 127.1, 126.7, 119.4, 119.4, 116.5, 113.9, 112.3, 106.2, 106.1, 59.9, 55.6, 50.8, 41.0, 36.7, 36.0, 32.7, 29.7, 29.6, 26.9, 20.6, 20.4, 19.3, 14.4, 12.4, 12.3; IR (KBr): 3304, 3016, 1640, 1485, 1217 cm^{-1}; ESI-MS *m/z*: 570 $(M+H)^+$; HRMS *m/z*calcd for $C_{35}H_{39}NO_6$ $(M+H)^+$ 570.2856, found 570.2849.

Methyl-4-(7-(sec-butyl)-2-(4-methylbenzoyl)benzofuran-5-yl)-2-methyl-5-oxo-1,4,5,6,7,8-hexahydroquinoline-3-carboxylate (**20**)

White solid, yield: 80%; mp: 121-122 °C;^{1}H NMR (400 MHz, DMSO-d_6) δ: 9.20 (s, 1H), 7.90 (d, 2H, *J* = 8.0 Hz), 7.68 (s, 1H), 7.38 (d, 2H, *J* = 8.0 Hz), 7.33 (s, 1H), 7.26 (d, 1H, *J* = 1.4 Hz), 5.01 (s, 1H), 3.53 (s, 3H), 3.13-3.04 (m, 1H), 2.50-2.49 (m, 2H), 2.41 (s, 3H), 2.30 (s, 3H), 2.23-2.15 (m, 2H), 1.94-1.66 (m, 4H), 1.30 (t, 3H, *J* = 7.2 Hz), 0.79 (t, 3H, *J* = 7.2 Hz); ^{13}C NMR (100 MHz, $CDCl_3$) : 196.1, 184.2, 168.1, 153.5, 153.4, 152.3, 152.2, 150.6, 143.8, 134.8, 131.3, 129.8, 129.2, 127.4, 127.0, 126.9, 126.8, 119.1, 117.1, 117.0, 113.3, 105.8, 105.7, 51.0, 37.1, 36.4, 36.3, 35.8, 29.6, 27.3, 21.7, 21.1, 20.5, 20.4, 19.2, 12.2, 12.1; IR (KBr): 3273, 3080, 1678, 1479, 1210 cm^{-1}; ESI-MS *m/z*: 512 $(M+H)^+$; HRMS *m/z*calcd for $C_{32}H_{33}NO_5$ $(M+H)^+$ 512.2437, found 512.2432.

Ethyl-4-(7-(sec-butyl)-2-(4-methylbenzoyl)benzofuran-5-yl)-2-methyl-5-oxo-1,4,5,6,7,8-hexa hydroquinoline-3-carboxylate (**21**)

White solid, yield: 80%; mp: 203-204 °C;^{1}H NMR (500 MHz, DMSO-d_6) δ: 9.17 (s, 1H), 7.90 (d, 2H, *J* = 8.0 Hz), 7.70 (d, 1H, *J* = 2.9 Hz), 7.39 (d, 2H, *J* = 6.2 Hz), 7.35 (s, 1H), 7.28 (s, 1H), 5.01 (s, 1H), 4.00-3.96 (m, 2H), 3.11-3.05 (m, 1H), 2.50 (brs, 2H), 2.42 (s, 3H), 2.30 (s, 3H), 2.25-2.19 (m, 2H), 1.92-1.71 (m, 4H), 1.33-1.30 (m, 3H), 1.14 (t, 3H, *J* = 7.0 Hz), 0.80 (t, 3H, *J* = 7.2 Hz); ^{13}C NMR (100 MHz, $CDCl_3$) : 195.9, 184.2, 167.6, 153.4, 152.3,

150.2, 143.9, 143.7, 134.9, 131.3, 131.2, 129.8, 129.3, 127.5, 127.3, 126.9, 119.4, 116.9, 113.5, 106.2, 59.9, 37.1, 36.5, 36.4, 36.0, 29.8, 29.6, 27.4, 21.8, 21.2, 20.5, 20.4, 19.3, 14.4, 12.3, 12.2; IR (KBr): 3390, 3079, 1694, 1434, 1230 cm^{-1}; ESI-MS *m/z*: 526 $(M+H)^+$; HRMS *m/z*calcd for $C_{33}H_{35}NO_5$ $(M+H)^+$ 526.2593, found 526.2595.

*Methyl-4-(7-(sec-butyl)-2-(4-methylbenzoyl)benzofuran-5-yl)-2,7,7-trimethyl-5-oxo-1,4,5,6, 7,8-hexahydroquinoline-3-carboxylate (***22***)*

White solid, yield: 80%; mp: 201-202 °C;^{1}H NMR (500 MHz, DMSO-d_6) δ: 9.15 (s, 1H), 7.90 (d, 2H, *J* = 8.0 Hz), 7.69 (s, 1H), 7.38 (d, 2H, *J* = 8.0 Hz), 7.30 (d, 1H, *J* = 8.0 Hz), 7.24 (d, 1H, *J* = 1.4 Hz), 5.01 (s, 1H), 3.55 (s, 3H), 3.12-3.04 (m, 1H), 2.50-2.49 (m, 2H), 2.42 (s, 3H), 2.29 (s, 3H), 1.74-1.66 (m, 4H), 1.31-1.28 (m, 3H), 0.99 (s, 3H), 0.89 (s, 3H), 0.78-0.75 (m, 3H); ^{13}C NMR (100 MHz, $CDCl_3$) : 201.0, 184.2, 168.2, 153.5, 153.4, 152.2, 148.4, 144.2, 143.7, 134.9, 131.4, 129.8, 129.2, 127.2, 126.8, 119.0, 117.2, 117.1, 111.8, 105.3, 51.1, 40.2, 36.6, 35.8, 34.8, 29.7, 29.6, 25.2, 24.4, 24.0, 21.8, 20.5, 19.4, 12.3, 12.1; IR (KBr): 3319, 3019, 1645, 1472, 1214 cm^{-1}; ESI-MS *m/z*: 540 $(M+H)^+$; HRMS *m/z*calcd for $C_{34}H_{37}NO_5$ $(M+H)^+$ 540.2750, found 540.2759.

Methyl-4-(7-(sec-butyl)-2-(4-chlorobenzoyl)benzofuran-5-yl)-2-methyl-5-oxo-1,4,5,6,7,8-hex ahydroquinoline-3-carboxylate (**23**)

White solid, yield: 80%; mp: 155-156 °C;^{1}H NMR (500 MHz, DMSO-d_6) δ: 9.20 (s, 1H), 7.99 (d, 2H, *J* = 8.5 Hz), 7.73 (s, 1H), 7.65 (d, 2H, *J* = 8.5 Hz), 7.33 (d, 1H, *J* = 1.1 Hz), 7.28 (d, 1H, *J* = 1.6 Hz), 5.01 (s, 1H), 3.53 (s, 3H), 3.13-3.05 (s, 1H), 2.50-2.49 (m, 2H), 2.30 (s, 3H), 2.29-2.15 (m, 2H), 1.94-1.65 (m, 4H), 1.32-1.28 (m, 3H), 0.80-0.77 (m, 3H); ^{13}C NMR (100 MHz, $CDCl_3$) : 196.1, 184.24, 184.22 168.1, 153.52, 153.46, 152.3, 152.2, 150.7, 143.8, 134.8, 135.7, 131.4, 129.8, 129.3, 127.4, 127.1, 126.9, 126.8, 119.2, 117.1, 117.0, 113.4, 105.8, 105.7, 51.1, 37.2, 36.4, 36.37, 36.32, 35.8, 29.7, 27.3, 21.8, 21.2, 20.5, 19.2, 12.3,

12.1; IR (KBr): 3387, 3083, 1668, 1443, 1222 cm^{-1}; ESI-MS *m/z*: 533 $(M+H)^+$; HRMS *m/z*calcd for $C_{31}H_{30}ClNO_5$ $(M+H)^+$532.1891, found 532.1889.

Ethyl-4-(7-(sec-butyl)-2-(4-chlorobenzoyl)benzofuran-5-yl)-2-methyl-5-oxo-1,4,5,6,7,8-hexahydroquinoline-3-carboxylate (**24**)

White solid, yield: 81%; mp: 239-240 °C;^{1}H NMR (400 MHz, DMSO-d_6) δ: 9.17 (s, 1H), 7.99 (d, 2H, *J* = 8.6 Hz), 7.74 (s, 1H), 7.65 (d, 2H, *J* = 8.6 Hz), 7.34 (d, 1H, *J* = 1.6 Hz), 7.29 (s, 1H), 5.00 (s, 1H), 4.00-3.95 (m, 2H), 3.12-3.06 (m, 1H), 2.50-2.49 (m, 2H), 2.29 (s, 3H), 2.23-2.14 (m, 2H), 1.94-1.68 (m, 4H), 1.32-1.29 (m, 3H), 1.12 (t, 3H, *J* = 7.0 Hz), 0.79 (t, 3H, *J* = 7.3 Hz); ^{13}C NMR (100 MHz, $CDCl_3$) : 196.0, 183.0, 167.6, 153.6, 153.6, 151.9, 150.4, 144.1, 143.7, 139.3, 135.7, 131.4, 131.1, 128.9, 127.9, 127.6, 126.8, 126.7, 119.5, 117.3, 117.3, 113.4, 106.2, 59.9, 37.1, 36.6, 36.1, 29.8, 29.6, 27.4, 21.2, 20.5, 20.4, 19.3, 14.4, 12.3, 12.2; IR (KBr): 3362, 3083, 1668, 1443, 1222 cm^{-1}; ESI-MS *m/z*: 547 $(M+H)^+$HRMS *m/z*calcd for $C_{32}H_{32}ClNO_5$ $(M+H)^+$ 546.2047, found 546.2045.

Methyl-4-(7-(sec-butyl)-2-(4-chlorobenzoyl)benzofuran-5-yl)-2,7,7-trimethyl-5-oxo-1,4,5,6, 7,8-hexahydroquinoline-3-carboxylate (**25**)

White solid, yield: 84%; mp: 210-211 °C;^{1}H NMR (400 MHz, DMSO-d_6) δ: 9.16 (s, 1H), 7.99 (d, 2H, *J* = 8.6 Hz), 7.74 (s, 1H), 7.65 (d, 2H, *J* = 8.6 Hz), 7.30 (d, 1H, *J* = 1.5 Hz), 7.26 (d, 1H, *J* = 1.5 Hz), 5.01 (s, 1H), 3.55 (s, 3H), 3.12-3.04 (m, 1H), 2.50-2.49 (m, 2H), 2.30 (s, 3H), 1.74-1.65 (m, 4H), 1.29 (t, 3H, *J* = 7.1 Hz), 0.99 (s, 3H), 0.88 (s, 3H), 0.78-0.74 (m, 3H); ^{13}C NMR (100 MHz, $CDCl_3$) : 200.9, 183.02, 183.00, 168.1, 153.6, 151.9, 148.2, 148.1, 144.0, 143.9, 139.3, 135.8, 131.5, 131.5, 131.1, 128.9, 127.6, 127.2, 126.7, 126.6, 119.1, 117.5, 117.4, 111.9, 105.4, 51.1, 40.3, 36.7, 36.5, 35.9, 34.8, 29.8, 29.7, 25.2, 24.4, 24.2, 20.5, 19.5, 12.3, 12.2; IR (KBr): 3370, 3020, 1620, 1467, 1215 cm^{-1}; ESI-MS *m/z*: 561 $(M+H)^+$; HRMS *m/z*calcd for $C_{33}H_{34}ClNO_5$ $(M+H)^+$ 560.2204, found 560.2210.

Methyl-4-(7-(sec-butyl)-2-(4-nitrobenzoyl)benzofuran-5-yl)-2-methyl-5-oxo-1,4,5,6,7,8-hexa hydroquinoline-3-carboxylate (**26**)

White solid, yield: 80%; mp: 220-221 °C;^{1}H NMR (500 MHz, DMSO-d_6) δ: 9.20 (s, 1H), 8.38 (d, 2H, *J* = 8.8 Hz), 8.18 (d, 2H, *J* = 8.8 Hz), 7.78 (s, 1H), 7.34 (d, 1H, *J* = 1.2 Hz), 7.30 (d, 1H, *J* = 1.6 Hz), 5.01 (s, 1H), 3.53 (s, 3H), 3.12-3.06 (m, 1H), 2.50-2.49 (m, 2H), 2.29 (s, 3H), 2.23-2.15 (m, 2H), 1.94-1.67 (m, 4H), 1.32-1.29 (m, 3H), 0.80-0.77 (m, 3H); ^{13}C NMR (100 MHz, $CDCl_3$) : 195.9, 182.3, 167.9, 153.9, 153.9, 151.5, 150.3, 150.1, 144.2, 144.1, 143.9, 142.5, 131.6, 130.5, 128.3, 127.9, 126.8, 123.7, 119.5, 118.2, 113.5, 106.0, 51.1, 37.1, 36.6, 36.4, 35.9, 29.7, 27.5, 21.2, 20.4, 19.4, 12.3; IR (KBr): 3299, 3020, 1555, 1461, 1652, 1212 cm^{-1}; ESI-MS *m/z*: 543 $(M+H)^+$; HRMS *m/z*calcd for $C_{31}H_{30}N_2O_7$ $(M+H)^+$ 543.2131, found 543.2127.

Ethyl-4-(7-(sec-butyl)-2-(4-nitrobenzoyl)benzofuran-5-yl)-2-methyl-5-oxo-1,4,5,6,7,8-hexa hydroquinoline-3-carboxylate (**27**)

White solid, yield: 80%; mp: 236-237 °C;^{1}H NMR (500 MHz, DMSO-d_6) δ: 9.17 (s, 1H), 8.38 (d, 2H, *J* = 8.8 Hz), 8.19 (d, 2H, *J* = 8.8 Hz), 7.79 (s, 1H), 7.35 (d, 1H, *J* = 1.6 Hz), 7.31 (s, 1H), 5.00 (s, 1H), 3.99-3.95 (m, 2H), 3.12-3.06 (m, 1H), 2.50-2.49 (m, 2H), 2.29 (s, 3H), 2.22-2.14 (m, 2H), 1.93-1.66 (m, 4H), 1.31 (t, 3H, *J* = 5.9 Hz), 1.12 (t, 3H, *J* = 7.1 Hz), 0.79 (t, 3H, *J* = 7.1 Hz); ^{13}C NMR (100 MHz, $CDCl_3$) : 195.9, 182.3, 167.5, 153.9, 153.8, 151.5, 150.1, 149.9, 144.3, 143.5, 142.5, 131.5, 131.4, 130.6, 128.5, 128.2, 126.7, 126.6, 123.7, 119.7, 118.2, 118.1, 113.6, 106.3, 106.3, 59.9, 37.1, 36.6, 36.5, 36.2, 29.8, 29.6, 27.5, 21.2, 20.5, 20.4, 19.4, 14.4, 14.3, 12.3, 12.2; IR (KBr): 3250, 3023, 1637, 1567, 1428, 1273 cm^{-1}; ESI-MS *m/z*: 557 $(M+H)^+$; HRMS *m/z*calcd for $C_{32}H_{32}N_2O_7$ $(M+H)^+$ 557.2288, found 557.2283.

Methyl-4-(7-(sec-butyl)-2-(4-nitrobenzoyl)benzofuran-5-yl)-2,7,7-trimethyl-5-oxo-1,4,5,6,7,8-hexahydroquinoline-3-carboxylate (**28**)

White solid, yield: 80%; mp: 225-226 °C;^{1}H NMR (500 MHz, DMSO-d_6) δ: 9.16 (s, 1H), 8.38 (d, 2H, J = 8.8 Hz), 8.18 (d, 2H, J = 8.8 Hz), 7.78 (s, 1H), 7.32 (d, 1H, J = 1.5 Hz), 7.28 (d, 1H, J = 1.3 Hz), 5.01 (s, 1H), 3.54 (s, 3H), 3.13-3.06 (m, 1H), 2.50-2.49 (m, 2H), 2.30 (brs, 3H), 1.76-1.66 (m, 4H), 1.31-1.28 (m, 3H), 0.99 (s, 3H), 0.88 (s, 3H), 0.78-0.74 (m, 3H); ^{13}C NMR (100 MHz, $CDCl_3$) : 200.9, 182.3, 182.3, 168.1, 153.9, 153.8, 151.4, 150.1, 148.3, 148.2, 144.1, 144.08, 144.02, 142.6, 131.6, 130.5, 128.2, 127.8, 126.6, 126.5, 123.7, 119.4, 119.4, 118.4, 118.4, 111.7, 105.3, 51.1, 40.2, 36.7, 36.6, 35.9, 34.8, 29.7, 29.6, 25.2, 24.4, 24.2, 20.5, 20.4, 19.5, 12.3, 12.1; IR (KBr): 3318, 3015, 1644, 1540, 1495, 1229 cm^{-1}; ESI-MS *m/z*: 571 $(M+H)^+$; HRMS *m/z*calcd for $C_{33}H_{34}N_2O_7$ $(M+H)^+$ 571.2444, found 571.2449.

Methyl-4-(7-(tert-butyl)-2-(4-methoxybenzoyl)benzofuran-5-yl)-2-methyl-5-oxo-1,4,5,6,7,8-hexahydroquinoline-3-carboxylate (**29**)

White solid, yield: 80%; mp: 240-241 °C; ^{1}H NMR (400 MHz, DMSO-d_6) δ: 9.22 (s, 1H), 8.03 (d, 2H, J = 8.8 Hz), 7.68 (s, 1H), 7.35-7.33 (m, 2H), 7.11 (d, 2H, J = 8.8 Hz), 5.03 (s, 1H), 3.88 (s, 3H), 3.56 (s,3H), 2.50 (brs, 2H), 2.30 (s, 3H), 2.24-2.21 (m, 2H), 1.96-1.90 (m, 2H), 1.44 (s, 9H); ^{13}C NMR (100 MHz, $CDCl_3$) : 196.2, 182.9, 168.1, 163.6, 153.2, 152.4, 151.1, 144.3, 143.3, 135.01, 132.1, 130.0, 127.6, 125.8, 119.3, 115.9, 113.9, 113.2, 105.8, 55.6, 51.1, 37.1, 36.2, 34.3, 30.0, 27.3, 21.2, 19.2; IR (KBr): 3220, 3019, 1646, 1481, 1218 cm^{-1}; ESI-MS *m/z*: 528 $(M+H)^+$; HRMS *m/z* calcd for $C_{33}H_{33}NO_6$ $(M+H)^+$ 528.2386, found 528.2390.

Ethyl-4-(7-(tert-butyl)-2-(4-methoxybenzoyl)benzofuran-5-yl)-2-methyl-5-oxo-1,4,5,6,7,8-hexahydroquinoline-3-carboxylate (**30**)

White solid, yield: 82%; mp: 224-225 °C;^{1}H NMR (400 MHz, DMSO-d_6) δ: 9.19 (s, 1H), 8.03 (d, 2H, J = 8.8 Hz), 7.68 (s, 1H), 7.35 (brs, 2H), 7.11 (d, 2H, J = 8.8 Hz), 5.01 (s, 1H), 4.02-3.97 (m, 2H), 3.87 (s, 3H), 2.52-2.49 (m, 2H), 2.29 (s, 3H), 2.24-2.19 (m, 2H), 1.94-

1.77 (m, 2H), 1.45 (s, 9H), 1.13 (t, 3H, *J* = 7.0 Hz); ^{13}C NMR (100 MHz , $CDCl_3$) : 196.1, 182.9, 167.7, 163.6, 153.2, 152.5, 150.8, 143.9, 143.6, 134.8, 132.1, 130.0, 127.6, 126.1, 119.6, 115.9, 113.9, 106.3, 59.9, 55.6, 37.1, 36.5, 34.3, 30.0, 21.2, 19.3, 14.4; IR (KBr): 3383, 3020, 1659, 1470, 1216 cm^{-1}; ESI-MS *m/z*: 542 $(M+H)^+$; HRMS *m/z*calcd for $C_{33}H_{35}NO_6$ $(M+H)^+$ 542.2543, found 542.2545.

Methyl-4-(7-(tert-butyl)-2-(4-methoxybenzoyl)benzofuran-5-yl)-2,7,7-trimethyl-5-oxo-1,4,5,6, 7,8-hexahydroquinoline-3-carboxylate (**31**)

White solid, yield: 80%; mp: 201-202 °C;^{1}H NMR (400 MHz, DMSO-d_6) δ: 9.17 (s, 1H), 8.03 (d, 2H, *J*=8.8 Hz), 7.69 (s, 1H), 7.36-7.34 (m, 2H), 7.11 (d, 2H, *J*=8.8 Hz), 4.98 (s, 1H), 3.87 (s, 3H), 3.55 (s, 3H), 2.50-2.31 (m, 5H), 2.27-1.96 (m, 2H), 1.42 (s, 9H), 1.01 (s, 3H), 0.84 (s, 3H); ^{13}C NMR (100 MHz, $CDCl_3$) : 195.8, 182.9, 168.1, 163.6, 153.2, 152.4, 149.0, 144.4, 143.1, 135.1, 132.1, 130.1, 127.4, 125.6, 119.4, 116.1, 113.8, 112.2, 105.9, 55.6, 51.1, 40.9, 36.4, 34.3, 32.7, 29.7, 26.9, 19.4; IR (KBr): 3228, 3038, 1665, 1467, 1273 cm^{-1}; ESI-MS *m/z*: 556 $(M+H)^+$; HRMS *m/z*calcd for $C_{34}H_{37}NO_6$ $(M+H)^+$ 556.2699, found 556.2705.

Ethyl-4-(7-(tert-butyl)-2-(4-methoxybenzoyl)benzofuran-5-yl)-2,7,7-trimethyl-5-oxo-1,4,5,6, 7,8-hexahydroquinoline-3-carboxylate(**32**)

White solid, yield: 85%; mp: 125-126 °C; ^{1}H NMR (400 MHz, DMSO-d_6) δ: 9.14 (s, 1H), 8.03 (d, 2H, *J* = 8.8 Hz), 7.70 (s, 1H), 7.38 (d, 1H, *J* = 1.2 Hz), 7.33 (s, 1H), 7.11 (d, 2H, *J* = 8.8 Hz), 4.96 (s, 1H), 4.02-3.96 (m, 2H), 3.87 (s, 3H), 2.50-2.27 (m, 5H), 2.21-1.95 (m, 2H), 1.43 (s, 9H), 1.15 (t, 3H, *J* = 7.1 Hz), 1.01 (s, 3H), 0.85 (s, 3H); ^{13}C NMR (100 MHz, $CDCl_3$) : 195.8, 182.9, 167.6, 163.6, 153.2, 152.4, 148.8, 143.9, 143.3, 134.9, 132.1, 130.1, 127.4, 125.8, 119.7, 116.0, 113.8, 112.3, 106.2, 59.9, 55.6, 50.8, 41.0, 36.6, 34.3, 32.8, 30.0, 29.7, 26.9, 19.4, 14.4; IR (KBr): 3390, 3074, 1691, 1440, 1268 cm^{-1}; ESI-MS *m/z*: 570 $(M+H)^+$;HRMS *m/z*calcd for $C_{35}H_{39}NO_6$ $(M+H)^+$ 570.2856, found 570.2849.

5.6 Typical method for the preparation of 33 and 34

General synthetic procedure for preparation of ethyl 2-methyl-5-oxo-4-phenyl-1,4,5,6,7,8-hexahydroquinoline-3-carboxylate (**33**)

To a solution of benzaldehyde (1.0 mmol) in 5 mL ethanol were added ethyl acetoacetate (1.0 mmol), 1,3-cyclohexadione (1.0 mmol), ammonium acetate (3.0 mmol), and 5 mL glacial acetic acid. The reaction mixture was continued under reflux condition for 8 h. After completion of reaction (monitored by TLC), the reaction mixture was cooled to room temperature. The solid thus obtained was filtered and subjected to column chromatography with ethylacetate-hexane (20:80, v/v) furnishing **33** as a white solid (Scheme 2).

Ethyl 2-methyl-5-oxo-4-phenyl-1,4,5,6,7,8-hexahydroquinoline-3-carboxylate (**33**)

White solid, yield: 80%; mp: 241-242 °C;^{1}H NMR (400 MHz, DMSO-d_6) δ: 9.11 (s, 1H), 7.19-7.13 (m, 4H), 7.07-7.04 (m, 1H), 4.85 (s, 1H), 3.99-3.94 (m, 2H), 2.50-2.26 (m, 4H), 2.18-2.14 (s, 1H), 1.99-1.95 (m, 1H), 1.14-1.10 (t, 3H, J = 8 Hz), 1.00 (s, 3H), 0.84 (s, 3H);^{13}C NMR (100 MHz, $CDCl_3$) : 194.6, 166.9, 151.4, 147.7, 144.8, 127.8, 127.3, 125.6, 111.0, 103.5, 59.0, 36.7, 35.6, 26.1, 20.7, 18.2, 14.1; IR (KBr): 3342, 2978, 1690, 1215 cm^{-1}; ESI-MS: m/z: 312 $(M+H)^+$; HRMS (*m/z*): calcd. for $C_{19}H_{21}NO_3$ $(M+H)^+$ 312.1610, found 312.1615.

Ethyl 2,7,7-trimethyl-5-oxo-4-phenyl-1,4,5,6,7,8-hexahydroquinoline-3-carboxylate(**34**)

White solid, yield: 80%; mp: 219-220 °C; ^{1}H NMR (400 MHz, DMSO-d_6) δ: 9.11 (s, 1H), 7.19-7.13 (m, 4H), 7.08-7.04 (m, 1H), 4.89 (s, 1H), 4.00-3.95 (m, 2H), 2.50-2.46 (m, 2H), 2.27 (s, 3H), 2.21-2.16 (m, 2H), 1.92-1.77 (m, 1H), 1.74-1.69 (m, 1H), 1.14-1.10 (t, 3H, J = 8 Hz), 1.00 (s, 3H), 0.84 (s, 3H);^{13}C NMR (100 MHz, $CDCl_3$) 194.2, 166.8, 149.4, 147.6, 144.9, 127.6, 127.4, 125.6, 109.9, 103.6, 59.0, 50.2, 35.8, 32.1, 29.1, 26.4, 18.2, 14.1; IR (KBr): 3050, 2950, 1700, 1230 cm^{-1}; ESI-MS: m/z: 340 $(M+H)^+$; HRMS (*m/z*): calcd. for $C_{21}H_{25}NO_3$ $(M+H)^+$ 339.1834, found 339.1840.

5.7 Biological Methods.

5.7.1 Isolation of rat calvarial osteoblasts for in-vitro studies

All experiments were executed in accordance with IAEC (Institutional Animal Ethical Committee, New Delhi, Ref. No. IAEC/2013/17) guidelines.Calvarial osteoblasts were isolated from 1 to 2 day old rats' pups. Calvariawere surgically separated from the skull and cleaned to remove the adherent tissue. Collective calvaria were kept for repeated digestion (15 min. /digestion) with 0.1% dispase 0.1% collagenase P to release osteoblasts cells from tissue. The cells from first digestion were discarded and from subsequent 4 digestions were collected and cultured in minimum essential media (α-MEM), supplemented with 10% fetalcalf serum (FCS) and 1% penicillin/streptomycin. Cultures of rat calvarial osteoblasts were allowed to reach confluences of 70- 80% for further experiments [52].

5.7.2 . Alkaline phosphatase (ALP) assay

Bone specific alkaline phosphatase (ALP) enzyme is a glycoprotein that is membrane bound exoenzyme of osteoblasts. ALP activity represents increased bone formation ability of the osteoblasts and is widely recognized as a biochemical marker for osteoblast activity in screening to select the lead compound when large number of compounds is to be screened. In- brief, 70%-80% confluences calvarial osteoblasts were trypsinized and 2x1000 cells/well were seeded in 96 wells plate. Cells were treated with different concentrations of the test compound or vehicle for 48 hour in growth medium supplemented with 10 mM β-glycerophosphate and 50 µg/mL ascorbic acid (osteoblasts differentiation medium). At the end, ALP activity was measured using *p*-nitrophenyl phosphate as substrate and absorbance was read at 405 nm. Alkaline phosphatase is a differentiation marker of osteoblast. The improved method utilizes *p*-nitrophenyl phosphate that is hydrolyzed by ALP in differentiated osteoblast into a yellow coloured product at alkaline pH (maximal absorbance

at 405nm). The rate of the reaction is directly proportional to the enzyme activity which itself is proportional to osteoblast differentiation [52].

5.7.3 Mineralization of Calvarial Osteoblasts

Mineralization of bone is essential for bone hardness, strength and involves a well-organized process in which crystals of calcium phosphate is developed by bone-forming cells that lay down in precise amounts within the bone's fibrous matrix or scaffold. Therefore, we examined mineralization ability for the most active compounds at different concentrations. In-brief, Rat calvarial osteoblasts were seeded in 12-wells plate in osteoblasts differentiation medium ($1x10^4$cells/well). The treatment group contained similar medium but supplemented with synthesized compound at different active concentrations. The media were changed every alternate days and cells cultured for twenty-one days. At the end of the treatment period, cells were washed with PBS and fixed with 4% paraformaldehyde in PBS for 15 min. The fixed cells were stained with 40 mM Alizarin-red (pH-4.5) stain for 30 min followed by washing with tap water. The mineralization was tested only for some selected compounds (8, 9, 14, 16 and 21) which had positive effect on ALP activity. For the quantification of Alizarin red stain 800 µL of 10% (v/v), acetic acid was added to each well, and plates were incubated at room temperature for 30 min with shaking. After incubationtime, cells in each well was scraped with a cell scraper and collected in separate vial then overlayed with 50 µL of mineral oil. The slurry was heated to 85°C for 5 min and then collected in ice. The slurry was then centrifuged at 1200 rpm for 15 min and 500 µLsupernatant collected in a separate tube, 200 µL of 10% NH_4OH was added and absorbance was taken at 405 nm [52].

5.7.4 Quantitative Real-Time Polymerase Chain Reaction (qRT-PCR)

Cells were seeded and treated with active concentrations of the screened compounds for 48 hour. Cells were homogenized and collected in TRIzol (Invitrogen) and total RNA was

extracted according to the manufacturer's protocol. The concentration and purity of isolated RNA were determined by quantifying the absorbance at 260 nm (A260) and the ratio of the absorbance at 260 nm to 280 nm (A260/A280), individually. cDNA was synthesized using kit (Thermo Scientific, USA) as given in manufacturers protocol from 2µg of RNA extracted from different groups bones. SYBR green (pure gene, genetix) was used for quantitative determination of the mRNAs of different genes. The design of forward and reverse primers was based on previous published cDNA sequences using the universal probe library (Roche Diagnostics, USA). For real-time PCR study, cDNA was amplified through Light Cycler 480 (Roche Diagnostics Pvt. Ltd). The temperature summary of the reaction was first 95°C for 5 min, 45 cycles of denaturation at 94°C for 2 min, annealing extension at 62°C for 30 s and extension at 72°C for 30 s. *Glyceraldehydes 3-phosphate dehydrogenase (GAPDH)* was used to a control to normalize differences in RNA isolation, and difference between efficiencies of the reverse transcription. Quantitative real-time PCR reaction was performed for determination of the relative expression of transcripts of osteoblastogenic genes *Runt-related transcription factor 2(RUNX2), Alkaline phosphatase (ALP), Collagen type-I (COL1), Bone morphogenetic protein 2(BMP2), Osterix*(*Osx*) using Light Cycler SYBR Green (Roche Diagnostics) according to manufacturer's instructions [53]. Primers were designed using Universal Probe Library for allgenes(**Table 3**).

Table 3: Primer sequence of various genes used for qPCR

Gene name	Primer sequence
Alp	F: GCA CAA CAT CAA GGA CAT CG R: TCA GTT CTG TTC TTG GGG TAC AT
Col-1	F: CAT GTT CAG CTT TGT GGA CCT R: GCA GCT GAC TTC AGG GAT GT
Osx	F: TGC CCC AC TGT CAG GAG R: GAT GTG GCG GCT GTG AAT
BMP-2	F: CGG ACT GCG GTC TCC TAA NM R: GGG GAA GCA GCA ACA CTA GA
Runx-2	F: CCA CAG AGC TAT TAA AGT GAC AGT G

	R: AAC AAA CTA GGT TTA GAG TCA TCA AGC
GAPDH	F:TTT GAT GTT AGT GGG GTC TCG R: AGC TTG TCA TCA ACG GGA AG

All primers were designed using Universal Probe Library for the above genes. alkaline phosphatase (*Alp*), osterix (*Osx*), collagen type-1 (*Col1*), runt-related transcription factor 2 (*Runx2*), bone morphogenic protein-2 (*Bmp2*) and glyceraldehyde-3-phosphate dehydrogenase (*GAPDH*)

5.7.5 Cell cytotoxicity assay

The toxicity of the synthesized compound **21** was tested on calvarial osteoblast cells. Cells were seeded in 96 well plates at 2000 cells/well in growth medium. Cells were treated with concentrations of 1 pMto 100 uM of compound **21** in differentiation medium for 48 h. The cell toxicity and viability in presence of synthesized compound were determined using MTT (3-(4, 5-dimethylthiazol-2-yl)-2, 5-diphenyltetrazolium bromide) assay [33].

5.7.6 BMP2 (Bone Morphogenetic Protein2) ELISA

BMPs are secreted signalling molecules and it is regulators of cartilage and bone formation. For the quantitative determination of BMP2 concentration inosteoblasts, 5 × 103 cells/well was seeded in 12-well plates. Cells were treated to lead compound **21** for 48 hours in α-MEM medium added with 1% charcoal-stripped FCS. At the end of incubation, supernatants were collected for determination of BMP2 by Elisa. In brief, 100 µL assay diluent then 50 µL of each standard, control and sample for 2 h on shaker. After this conjugate and substrate was added. Finally, reaction was terminated by stop solution and OD measured at 450 nm according to the manufacturer's instructions (R&D Systems DBP 200) [54].

5.7.7 Subcutaneous injection of compound 21 was used only for selecting best possible doses

In in-vitro studies normally used calvarial cells for finding any activity of test compound and for *in-vivo* dose determination we used subcutaneous injection of test compound at

calvarialskull site. For this study we gave injection of compound **21** (0.1, 0.5, 1.0, 5.0, 10 and 20 $mg.kg^{-1}day^{-1}$) given subcutaneously or equal volume of vehicle (normal saline) for 3 consecutive days in skull part. At the end of the experiments, calvarias were collected for RNA. Total RNA was isolated by trizol method and qRT-PCR for Runx2 and BMP2 was performed as described earlier [55].

5.7.8. In-vivo study of compound 21 in rapid fracture healing model by 0.8 mm diameter defect in femoral bone

Twelve adult female *Sprague−dawley*rats (200 ± 20 g each, 12 weeks old) were taken for the study. For general anesthesia, a ketamine (85 mg/kg) and xylazine (15 mg/kg) mixture was injected intraperitoneally. The left leg was shaved and sterilized with a disinfect solution. The front skin of the mid-femur in rats was incised anaesthetic condition. After splitting the muscle around the bone, we exposed the femur bone surface by stripped the periosteum bone surface. A rapid fracture healing model was developed by injury on bone by creating defect of 0.8 mm diameter in the anterior portion of the diaphysis of the femurs, above the knee joint. 0.8 mm size defect was made at 2 cm (2000 millimetres) above the knee joint from distal femur side and distance was measured by digital Verniercalipers for uniformly injury site in all animals. Treatments started from the next day of injury and continued for 14 days. For the various treatments, rats were divided into two equal groups (6 rats/group) as follows: vehicle (gum acacia in distilled water), and compound **21**(10 $mg.kg^{-1}.day^{-1}$) for 14 consecutive days. 2 days before autopsy, all animals received intra-peritoneal administration of fluorochromecalcein (20 $mg.kg^{-1}$). After 14 days all rats were euthanized and autopsied to collect their femur for the measurement of bone micro-architectural parameters at defect size by micro-CT (Sky Scan 1076). Femur bone tissue processing, scanning, and measurement of bone micro-architectural Parameters in the defected site was done by previously describe

method in this study with little modification. In brief, bone defect regions were scanned at an isotropic voxel size of 18 μm^3, at a voltage of 70 kV, a current of 142 mA, field of view of 35 mm, by using a 1.0 mm aluminium filter (For removing signal noise), over 360 degrees, 0.8-degree rotation step with full width. 3D images in defected region drawn by CT volume software by selecting ROI files of reconstructed scanned files and 2D images drawn with Data-viewer software. To analyze 3D parameters in fractured femurs, whole bone was scanned and reconstructed. The region of interest in fracture (defect) site was studied by drawing ellipsoid contours manually (initiation to end of fractured site where cortical bone was non-existent in selected region) with the CT analyzer software by total 50 slices. Analysis of various parameters was done by BATMAN software. The intensity of calcein binding, which is a marker of new mineral depositions at fracture region, was calculated using Carl Zeiss AM 4.2 image analysis software. For calceinlabeling intensity and callus regeneration at defect region studies by embedding bone in an acrylic material and Sections of 50 µM were made by an Isomet bone cutter, and photographs were taken under a confocal microscope (Carl Zeiss LSM 510 Meta) aided with suitable filters [56]. For H&E staining of callus site all bones were first decalcified in EDTA and stained. qRT-PCR analysis of BMP2 at callus site in fractured bone was performed by marked and cut the region having callus with the help of sharp blade by bone cutter (Isomet bone cutter, Buehler, Illinois USA). Three specimens of callus (300 µm proximal and distal to the fracture site) for both groups were harvested after autopsy. The harvested tissue was frozen in liquid nitrogen and stored at −80°C until it was used for RNA isolation. The specimens were powdered in liquid nitrogen using a mortar and pestle. Total RNA was extracted with Trizol (Invitrogen).

,

5.7.9. Histology of liver

At the time of animal's autopsy, liver tissue were dissected out and embedded in paraffin wax. For histo-morphometric analysis of the liver section of each group's animals was cut by

microtome (Leica RM2165) of 5 µm size. Sections were obtained on poly L-lysin coated glass slides. Paraffin sections were de-waxed re-hydrated by gradient of xylene/isopropanol and then were stained with haematoxylin and eosin (H&E). Photomicrographs of bone sections were obtained using microscope (CKX41 trinocular with cooled CCD Camera model Q imaging MP 5.0-RTV-CLR-10C from Olympus, Tokyo, Japan).

5.7.10. ***Statistical analysis***

Results were obtained from minimum three independent experiments in triplicate and are expressed as mean ± SEM. For significance, $P<0.05$ *was* used and in each group, results were reproducible and there were no disagreements amongst the blinded assessors. Comparisons of different parameters among all of the groups were analyzed through multiple comparison analysis within the groups using one-way ANOVA (non-parametric) and then a post hoc test "Newman-Keuls analysis" was applied using Prism software version 5.0. For in-vitro studies, culture of rat calvarial osteoblasts cells was used for ALP, mineralization, and MTT by using n=8 replicates. For study of gene expression analysis by qRT-PCR analysis n=3 replicates were taken. For in-vivo studies as rapid bone healing potential by drill hole defect measurement and calcein intensity measurement, n=6 animals (6 replicates) were taken in each experimental group.

6. Computational Methods

Docking studies were carried out with compound **8**, **9**, **14**, **16**, **21** and BMP2 protein, using PDB structure 3BK3. Binding sites for agonist binding on protein surface were predicted by using MetaPocket2.0 [57] and best site having highest Z score was subjected to docking studies using AutoDock 4.2 [58]. In docking studies, 100 poses were generated using long number of evaluations, and default docking parameters. Thereby, molecular level binding of agonist to its binding site was predicted. Structure of all compounds was built and minimized using MarvinSketch version 6.1.2 from ChemAxon [59] and energy minimized using

finebuild method. The pocket identified was docked with all compounds. Docking poses were visualized and images were processed by using Chimera 1.8.1 [60].

Acknowledgment

Instrumentation facilities from SAIF, CDRI are gratefully acknowledged. R.K.M., D.C., B.R.K, and S. G. are thankful to CSIR, New Delhi for financial support. Financial support from "BSC0201 (Anabolic Skeletal Targets in Health & Illness)" is acknowledged. We thankDr.Kavita Singh of EM unit, CSIR-central drug research institute for collecting confocal microscopy data reported in this paper and Dr.KalyanMitra for facilitating confocal imaging. We also acknowledge Mr. G.K. Nagar, for his support in histology. The authors are grateful to the Director, CDRI, Lucknow, India for constant encouragement in drug development program. This is CSIR-CDRI Communication No 174/2017/RT.

Additional Information-The authors declare no competing financial interests.

References

[1]. D.T. Sugerman, JAMA patient page. Osteoporosis, Jama 311 (2014) 104.

[2]. R.A. Adler, Osteoporosis in men: a review, Bone Res. 2 (2014) 14001.

[3]. National Osteoporosis Foundation. Available at: http://nof.org/nationalosteoporosismonth. (accessed 11.07.14).

[4]. H. Richard, Osteoporosis - striking the right balance. The Lancet 377 (**2011**) 2152.

[5]. E. Barrett-Connor, E.S. Siris, L.E. Wehren, P.D. Miller, T.A. Abbott, M.L. Berger, A.C. Santora, L.M. Sherwood, Osteoporosis and fracture risk in women of different ethnic groups, J. Bone Miner. Res. 20 (2005) 185-194.

[6]. E.S. Siris, P.D. Miller, E. Barrett-Connor, K.G. Faulkner, L.E. Wehren, T.A. Abbott, M.L. Berger, A.C. Santora, L.M. Sherwood, Identification and fracture outcomes of undiagnosed low bone mineral density in postmenopausal women: results from the National Osteoporosis Risk Assessment, JAMA 286 (2001) 2815-2822.

[7]. J.P. van den Bergh, T.A. van Geel, P.P. Geusens, Osteoporosis, frailty and fracture: implications for case finding and therapy, Nat. Rev. Rheumatol. 8 (2012) 163-172.

[8]. G.A. Rodan, T.J. Martin, Therapeutic approaches to bone diseases, Science 289 (2000) 1508-1514.

[9]. K. Akesson, New approaches to pharmacological treatment of osteoporosis, Bull. World Health Organ. 81 (2003) 657-664.

[10]. M. Kawai, U.I. Modder, S. Khosla, C.J. Rosen, Emerging therapeutic opportunities for skeletal restoration, Nat. Rev. Drug. Discov. 10 (2011) 141-156.

[11]. J.E. Mulder, N.S. Kolatkar, M.S. LeBoff, Drug insight: Existing and emerging therapies for osteoporosis, Nat. Clin. Pract. Endocrinol. Metab. 2 (2006) 670-680.

[12]. C. Berg, K. Neumeyer, P. Kirkpatrick, Teriparatide, Nat. Rev. Drug Discov. 2 (2003) 257-258.

[13]. V. Subbiah, V.S. Madsen, A.K. Raymond, R.S. Benjamin, J.A. Ludwig, Of mice and men: divergent risks of teriparatide-induced osteosarcoma, Osteoporos Int. 21 (2010) 1041-1045.

[14]. U. Yasothan, S. Kar, Osteoporosis: overview and pipeline, Nat. Rev. Drug Discov. 7 (2008) 725-726.

[15]. E.H. Riley, J.M. Lane, M.R. Urist, K.M. Lyons, J.R. Lieberman, Bone morphogenetic protein-2: biology and applications, Clin. Orthop. Relat. Res. (1996) 39-46.

[16]. M. Egermann, A.W. Baltzer, S. Adamaszek, C. Evans, P. Robbins, E. Schneider, C.A. Lill, Direct adenoviral transfer of bone morphogenetic protein-2 cDNA enhances fracture healing in osteoporotic sheep, Hum. Gene Ther. 17 (2006) 507-517.

[17]. W.F. McKay, S.M. Peckham, J.M. Badura, A comprehensive clinical review of recombinant human bone morphogenetic protein-2 (INFUSE Bone Graft), Int. Orthop. 31 (2007) 729-734.

[18]. R. Trivedi, R. Goswami, N. Chattopadhyay, Investigational anabolic therapies for osteoporosis, Expert Opin. Investig. Drugs 19 (2010) 995-1005.

[19]. M. Kamal, A. K. Shakya, T. Jawaid, Benzofurans: a new profile of biological activities, Int. J. Med. Pharm. Sci. 1 (2011) 1-15.

[20]. K.M. Dawood, Benzofuran derivatives: a patent review, Expert Opin. Ther. Pat. 23 (2013) 1133-1156.

[21]. B. Sekhar.; M. Khalid, L. David, Methods using chromene and benzofuran compounds for promoting joint and bone health. *PCT Int. Appl*. (2007) WO 2007139887 A2 20071206.

[22]. Y. Oishi, M. Koita, Compositions for treatment of metabolic bone diseases containing benzofuran derivatives. *Jpn. KokaiTokkyoKoho*(2006) JP 2006225303 A 20060831.

[23]. S. T. Xue, H.F. Guo, M. J. Liu, J. Jin, D.H. Ju, Z.Y. Liu, Z.R. Li.Synthesis of a novel class of substituted benzothiophene or benzofuran derivatives as BMP-2 up-regulators and evaluation of the BMP-2-up-regulating effects in vitro and the effects on glucocorticoid-induced osteoporosis in rats. Eur. J. Med. Chem. 96 (2015) 151-161.

[24]. S. A. Fontana, Benzofurans used to inhibit bone loss. (1996) US 5489587 A 19960206.

[25]. S. Kumar, L. Dare, J.A. Vasko-Moser, I.E. James, S.M. Blake, D.J. Rickard, S.M. Hwang, T. Tomaszek, D.S. Yamashita, R.W. Marquis, H. Oh, J.U. Jeong, D.F. Veber, M. Gowen, M.W. Lark, G. Stroup, A highly potent inhibitor of cathepsin K (relacatib) reduces biomarkers of bone resorption both in vitro and in an acute model of elevated bone turnover in vivo in monkeys, Bone 40 (2007) 122-131.

[26]. H.F. Guo, H.Y. Shao, Z.Y. Yang, S.T. Xue, X. Li, Z.Y. Liu, X.B. He, J.D. Jiang, Y.Q. Zhang, S.Y. Si, Z.R. Li, Substituted Benzothiophene or Benzofuran Derivatives as a Novel Class of Bone Morphogenetic Protein-2 Up-Regulators: Synthesis, Structure-Activity Relationships, and Preventive Bone Loss Efficacies in Senescence Accelerated Mice (SAMP6) and Ovariectomized Rats, J. Med. Chem. 53 (2010) 1819-1829.

[27]. S.E. Guggino, D. Lajeunesse, J.A. Wagner, S.H. Snyder, Bone remodeling signaled by a dihydropyridine- and phenylalkylamine-sensitive calcium channel, Proc. Natl. Acad. Sci. U S A 86 (1989) 2957-2960.

[28]. Y. Nishiya, S. Sugimoto, Effects of various antihypertensive drugs on the function of osteoblast, Biol. Pharm. Bull. 24 (2001) 628-633.

[29]. K.Y. Kang, Y. Kang, M. Kim, Y. Kim, H. Yi, J. Kim, H.R. Jung, S.H. Park, H.Y. Kim, J.H. Ju, Y.S. Hong, The Effects of Antihypertensive Drugs on Bone Mineral Density in Ovariectomized Mice, J. Korean Med. Sci. 28 (2013) 1139-1144.

[30]. M. Ghosh, S.R. Majumdar, Antihypertensive medications, bone mineral density, and fractures: a review of old cardiac drugs that provides new insights into osteoporosis, Endocrine. 46 (2014) 397-405.

[31]. B.X. Wang, M. Bi, Z. Zhu, L. Wu, J.Y. Wang, Effects of the antihypertensive drug benidipine on osteoblast function in vitro, Exp. Ther. Med. 7 (2014) 649-653.

[32]. K. Ushijima, Y.W. Liu, T. Maekawa, E. Ishikawa, Y. Motosugi, H. Ando, S. Tsuruoka, A. Fujimura, Protective effect of amlodipine against osteoporosis in stroke-prone spontaneously hypertensive rats, Eur. J. Pharmacol. 635 (2010) 227-230.

[33]. K.V. Sashidhara, M. Kumar, V. Khedgikar, P. Kushwaha, R.K. Modukuri, A. Kumar, J. Gautam, D. Singh, B. Sridhar, R. Trivedi, Discovery of Coumarin-Dihydropyridine Hybrids as Bone Anabolic Agents, J. Med. Chem. 56 (2013) 109-122.

[34]. K.V. Sashidhara, M. Kumar, R. Sonkar, B.S. Singh, A.K. Khanna, G. Bhatia, Indole-Based Fibrates as Potential Hypolipidemic and Antiobesity Agents, J. Med. Chem. 55 (2012) 2769-2779.

[35]. (a) K.V. Sashidhara, R.K. Modukuri, D. Choudhary, K.B. Rao, M. Kumar, V. Khedgikar, R. Trivedi, Synthesis and evaluation of new coumarin-pyridine hybrids with promising anti-osteoporotic activities, Eur. J. Med. Chem. 70 (2013) 802-810. (b) K.V. Sashidhara, S.R. Avula, V. Mishra, G.R. Palnati, L.R. Singh, N. Singh, Y.S. Chhonker, P. Swami, R.S. Bhatta, G. Palit, Identification of quinoline-chalcone hybrids as potential antiulcer agents, Eur. J. Med. Chem. 89 (2015) 638-653.

[36]. K.V. Sashidhara, M. Kumar, R.K. Modukuri, R.K. Srivastava, A. Soni, K. Srivastava, S.V. Singh, J.K. Saxena, H.M. Gauniyal, S.K. Puri, Antiplasmodial activity of novel keto-enaminechalcone-chloroquine based hybrid pharmacophores, Bioorg. Med. Chem. 20 (2012) 2971-2981.

[37]. C. Viegas-Junior, A. Danuello, V.D. Bolzani, E.J. Barreir, C.A.M. Fraga, Molecular hybridization: A useful tool in the design of new drug prototypes, Curr. Med. Chem. 14 (2007) 1829-1852.

[38]. J. Marco-Contelles, E. Soriano, "The Medicinal Chemistry of Hybrid-Based Drugs Targeting Multiple Sites of Action", Curr. Top. Med. Chem. 11 (2011) 2714-2715.

[39]. Y. Bansal, O. Silakari, Multifunctional compounds: Smart molecules for multifactorial diseases, Eur. J. Med. Chem. 76 (2014) 31-42.

[40]. (a) K.V. Sashidhara, R.K. Modukuri, R. Sonkar, K.B. Rao, G. Bhatia, Hybrid benzofuran-bisindole derivatives: New prototypes with promising anti-hyperlipidemic activities, Eur. J. Med. Chem. 68 (2013) 38-46. (b) K.V. Sashidhara, S.R. Avula, P.K. Doharey, L.R. Singh, V.M. Balaramnavar, J. Gupta, S. Misra-Bhattacharya, S. Rathaur, A.K. Saxena, J.K. Saxena, Designing, synthesis of selective and high-affinity chalcone-benzothiazole hybrids as Brugiamalayithymidylate kinase inhibitors: In vitro validation and docking studies, Eur. J. Med. Chem. 103 (2015) 418-428

[41]. (a) K.V. Sashidhara, M. Kumar, R.K. Modukuri, R. Sonkar, G. Bhatia, A.K. Khanna, S. Rai, R. Shukla, Synthesis and anti-inflammatory activity of novel biscoumarin-chalcone hybrids, Bioorg. Med. Chem. Lett. 21 (2011) 4480-4484. (b) K.V. Sashidhara, L.R. Singh, M. Shameem, S. Shakya, A. Kumar, T. S. Laxman, S. Krishna, M.I. Siddiqi, R.S. Bhatta, D. Banerjee, Design, synthesis and anticancer activity of dihydropyrimidinone–semicarbazone hybrids as potential human DNA ligase 1 inhibitors, MedChemComm, 7, (2016) 2349-2363.

[42]. J. R. Stille, J.A. Ward, C. Leffelman, K.A. Sullivan, 5-formyl salicylaldehyde as a linker for the synthesis of benzofuran containing insulin sensitivity enhancer compounds, Tetrahedron Lett. 37 (1996) 9267-9270.

[43]. D. Chen, M. Zhao, G.R. Mundy, Bone morphogenetic proteins, Growth factors 22 (2004) 233-241.

[44]. T.K. Sampath, J.E. Coughlin, R.M. Whetstone, D. Banach, C. Corbett, R.J. Ridge, E. Ozkaynak, H. Oppermann, D.C. Rueger, Bovine osteogenic protein is composed of dimers of OP-1 and BMP-2A, two members of the transforming growth factor-beta superfamily, J. Biol. Chem. 265 (1990) 13198-13205.

[45]. D. Weber, A. Kotzsch, J. Nickel, S. Harth, A. Seher, U. Mueller, W. Sebald, T.D. Mueller, A silent H-bond can be mutationally activated for high-affinity interaction of BMP-2 and activin type IIB receptor, BMC Struct. Biol. 7 (2007) 6.

[46]. W. Sebald, J. Nickel, J.L. Zhang, T.D. Mueller, Molecular recognition in bone morphogenetic protein (BMP)/receptor interaction, Biol. Chem. 385 (2004) 697-710.

[47]. W. Sebald, J. Nickel, J.L. Zhang, T.D. Mueller, Molecular recognition in bone morphogenetic protein (BMP)/receptor interaction, Biol. Chem. 385 (2004) 697-710.

[48]. R.N. Wang, J. Green, Z. Wang, Y. Deng, M. Qiao, M. Peabody, Q. Zhang, J. Ye, Z. Yan, S. Denduluri, O. Idowu, M. Li, C. Shen, A. Hu, R.C. Haydon, R. Kang, J. Mok, M.J. Lee, H.L. Luu, L.L. Shi, Bone Morphogenetic Protein (BMP) signaling in development and human diseases, Genes Dis. 1 (2014) 87-105.

[49]. C.J. Wu, H.K. Lu, Smad signal pathway in BMP-2-induced osteogenesis - a mini review, J. Dent. Sci. 3 (2008) 13-21.

[50]. M.S. Rahman, N. Akhtar, H.M. Jamil, R.S. Banik, S.M. Asaduzzaman, TGF-beta/BMP signaling and other molecular events: regulation of osteoblastogenesis and bone formation, Bone Res. 3 (2015).

[51]. G.Q. Chen, C.X. Deng, Y.P. Li, TGF-beta and BMP Signaling in Osteoblast Differentiation and Bone Formation, Int. J. Biol. Sci. 8 (2012) 272-288.

[52]. R. Trivedi, S. Kumara, A. Kumar, J.A. Siddiqui, G. Swarnkar, V. Gupta, A. Kendurker, A.K. Dwivedi, J.R. Romero, N. Chattopadhyay, Kaempferol has osteogenic effect in ovariectomized adult Sprague-Dawley rats, Mol. Cell Endocrinol. 289 (2008) 85-93.

[53]. P. Kumar, P. Kushwaha, V. Khedgikar, J. Gautam, D. Choudhary, D. Singh, R. Trivedi, R. Maurya, Neoflavonoids as potential osteogenic agents from Dalbergiasissoo heartwood, Bioorg. Med. Chem. Lett. 24 (2014) 2664-2668.

[54]. P. Kushwaha, V. Khedgikar, J. Gautam, P. Dixit, R. Chillara, A. Verma, R. Thakur, D. P. Mishra, D. Singh, R. Maurya, N. Chattopadhyay, P. R. Mishra, R. Trivedi, A novel therapeutic approach with Caviunin-based isoflavonoid that en routes bone marrow cells to bone formation via BMP2/Wnt-β-catenin signaling. Cell Death Differ. 5 (2014) e1422.

[55]. P. Kushwaha, V. Khedgikar, N. Ahmad, A. Karvande, J. Gautam, P. Kumar, R. Maurya, R. Trivedi, A neoflavonoiddalsissooal isolated from heartwood of DalbergiasissooRoxb. hasbone forming effects in mice model for osteoporosis, Eur. J. Pharmacol. 788 (2016) 65-74.

[56]. K. Sharan, J.S. Mishra, G. Swarnkar, J.A. Siddiqui, K. Khan, R. Kumari, P. Rawat, R. Maurya, S. Sanyal, N. Chattopadhyay, A novel quercetin analogue from a medicinal plant promotes peak bone mass achievement and bone healing after injury and exerts an anabolic effect on osteoporotic bone: the role of aryl hydrocarbon receptor as a mediator of osteogenic action, J. Bone Miner. Res. 26 (2011) 2096-2111.

[57]. W. Sebald, J. Nickel, J.L. Zhang, T.D. Mueller, Molecular recognition in bone morphogenetic protein (BMP)/receptor interaction, Biol. Chem. 385 (2004) 697-710.

[58]. Z. Zhang, Y. Li, B. Lin, M. Schroeder, B. Huang, Identification of cavities on protein surface using multiple computational approaches for drug binding site prediction, Bioinformatics 27 (2011) 2083-2088.

[59]. P. Ertl, Molecular structure input on the web, J. Cheminform. 2 (2010) 1.

[60]. G.M. Morris, R. Huey, W. Lindstrom, M.F. Sanner, R.K. Belew, D.S. Goodsell, A.J. Olson, AutoDock4 and AutoDockTools4: Automated docking with selective receptor flexibility, Journal of computational chemistry, 30 (2009) 2785-2791.

Graphical abstract